POINTWISE A POSTERIORI ERROR CONTROL FOR ELLIPTIC OBSTACLE PROBLEMS

RICARDO H. NOCHETTO, KUNIBERT G. SIEBERT, AND ANDREAS VEESER

ABSTRACT. We consider a finite element method for the elliptic obstacle problem over polyhedral domains in $\mathbb{R}^d$, which enforces the unilateral constraint solely at the nodes. We derive novel optimal upper and lower a posteriori error bounds in the maximum norm irrespective of mesh fineness and the regularity of the obstacle, which is just assumed to be Hölder continuous. They exhibit optimal order and localization to the non-contact set. We illustrate these results with simulations in 2d and 3d showing the impact of localization in mesh grading within the contact set along with quasi-optimal meshes.

1. INTRODUCTION

Let Ω be a bounded, polyhedral, not necessarily convex domain in $\mathbb{R}^d$ with $d \in \{1,2,3\}$. Let $f \in L^\infty(\Omega)$ be a load function, $\chi \in H^1(\Omega) \cap C^{0,\alpha}(\bar\Omega)$ be a lower obstacle, and $g \in H^1(\Omega) \cap C^{0,\alpha}(\bar\Omega)$ be a Dirichlet boundary datum with $0 < \alpha \le 1$. The last two functions satisfy the compatibility condition

$$g \ge \chi \quad \text{on } \partial\Omega.$$

Let $\mathcal{K}$ be the following non-empty, closed and convex set of $H^1(\Omega)$:

$$\mathcal{K} := \{v \in H^1(\Omega) \mid v \ge \chi \text{ a.e. in } \Omega \text{ and } v = g \text{ on } \partial\Omega\}.$$

The *continuous problem* reads as follows:

$$u \in \mathcal{K}: \qquad \langle \nabla u, \nabla(u-v)\rangle \le \langle f, u-v\rangle \qquad \text{for all } v \in \mathcal{K}. \tag{1.1}$$

It is well known that this problem admits a unique solution u; see e. g. [9, Theorem 6.2] or [8], [13]. Moreover, u is also Hölder continuous [7].

Let $\sigma \in H^{-1}(\Omega) = \mathring{H}^1(\Omega)^*$ be the non-positive functional defined by

$$\langle \sigma, \varphi\rangle = \langle f, \varphi\rangle - \langle \nabla u, \nabla\varphi\rangle \qquad \text{for all } \varphi \in \mathring{H}^1(\Omega). \tag{1.2}$$

Note that $\sigma = 0$ in the open *non-contact* set $\{u > \chi\} := \{x \in \Omega \mid u(x) > \chi(x)\}$, and that $\sigma = f + \Delta\chi$ in the interior of the *contact* set $\{u = \chi\}$.

Given a shape-regular partition $\mathcal{T}_h$ of Ω, we let (u_h, σ_h) be piecewise linear finite element approximations of (u, σ) over $\mathcal{T}_h$. The unilateral constraint is imposed on the discrete function u_h only at the nodes of $\mathcal{T}_h$. This corresponds to $u_h \ge \chi_h$, where χ_h is the Lagrange interpolant of χ. Since χ_h does not in general satisfy $\chi_h \ge \chi$, the ensuing method is *non-conforming*. Moreover, the discretization is such that the discrete counterpart $\sigma_h \le 0$ of $\sigma \le 0$ holds; see §2 for details.

Rigorous a posteriori error estimates in the energy norm have been recently derived by Chen and Nochetto [3] and Veeser [17, 18]. In [3] a global upper bound is

Date: November 12, 2001.

1991 *Mathematics Subject Classification.* 65N15, 65N30, 35J85.

Key words and phrases. elliptic obstacle problem, a posteriori error estimate, residual, maximum norm, maximum principle, barrier functions.

shown which hinges on a positivity preserving finite element interpolation operator Π_h; such a Π_h will also be instrumental here. In [17, 18] the interior residual is localized to the non-contact set, thereby sharpening the global upper estimate of [3] and producing a lower estimate [18]; localization will be essential here as well. The upper estimate guarantees *reliability* and the lower bound *efficiency*.

Before we embark on a formal discussion, it is instructive to pause on the standard approach for the Laplacian and compare it with (1.1). Since $-\Delta$ is an isomorphism between $\mathring{H}^1(\Omega)$ and its dual $H^{-1}(\Omega)$, we can simply write the equation satisfied by the discrete solution u_h in this case, namely $-\Delta u_h = f - \mathcal{R}_h =: \tilde{f}$, and thereby estimate the error $\|\nabla(u-u_h)\|_{0,2;\Omega}$ in terms of the residual $\|\mathcal{R}_h\|_{-1,2;\Omega} = \|f-\tilde{f}\|_{-1,2;\Omega}$. Hereafter, $\|\cdot\|_{0,p;\Omega}$ denotes the $L_p(\Omega)$-norm, $p \in [1,\infty]$, and $\|\cdot\|_{-1,2;\Omega}$ the dual norm of $\|\nabla\cdot\|_{0,2;\Omega}$. For the obstacle problem (1.1), the correspondence between right-hand side f and u is nonlinear, non-differentiable, and most notably not one-to-one since a change of f within the contact set $\{u=\chi\}$ may yield no change in u. This loss of information in u is accounted for in σ and, consequently, the pair (u,σ) is the relevant quantity for error analysis in the present context. This crucial observation was first made by Veeser [18] for the energy norm, and leads to both lower and upper bounds for the combined errors $u-u_h$ and $\sigma-\sigma_h$.

To understand the issues involved in deriving sharp pointwise a posteriori error estimates, it is revealing to consider simple one-dimensional situations. We thus resort to Figures 1.1-1.3, which were produced with the estimators of this paper. These pictures display three meshes together with discrete solutions (thin lines). The forbidden region below χ is shaded for ease of visualization and χ_h is shown by thick lines. Our estimators are consistent with those in [18] and thus control errors in u and σ with respect to the maximum norm and a negative Sobolev-type norm, respectively. An *optimal* error estimator and associated adaptive procedure should exhibit in particular the following basic properties (which are fulfilled for those of this paper):

- In the discrete contact set $\{u_h = \chi_h\}$ the estimator must be insensitive (apart from oscillations) to the forcing term f, which should not dictate mesh quality. Figures 1.1 and 1.2 illustrate this property since the meshes are rather coarse in the contact sets.
- In the non-contact set $\{u_h > \chi_h\}$ the estimator must be insensitive to the obstacle and thus reduce to the usual estimator for the (unconstrained) Laplacian. This effect is shown in Figures 1.1 and 1.2. The refinement in Figure 1.1 is due to the curvature generated by $f=-1$ but not to the cusp of χ pointing downwards. On the other hand, the estimator does not feel the oscillatory character of χ in Figure 1.2 because it takes place below the discrete solution u_h. Overall there is an excellent accuracy for u in the non-contact set even though the approximation of χ is rather rough.
- The estimator must be able to detect the non-conforming situation $\chi > u_h$, and refine accordingly. This is depicted in Figure 1.3, where the concave part of χ above u_h is detected early on and thereby the solution is lifted up.
- If $\sigma = f + \Delta u$ happens to be singular with respect to the Lebesgue measure, as in Figure 1.1, then we could expect a strong refinement near the discrete free boundary. In fact, the piecewise linear approximation σ_h of σ cannot be very accurate in such a case no matter whether the corresponding singularity in the exact solution u can be resolved in the discrete space.

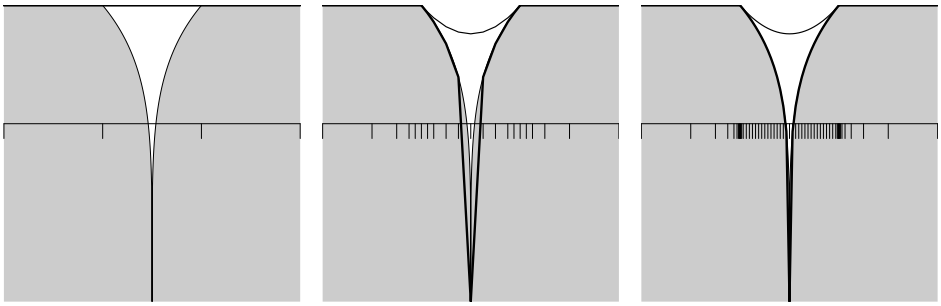

FIGURE 1.1. Localization for an obstacle with downward cusp

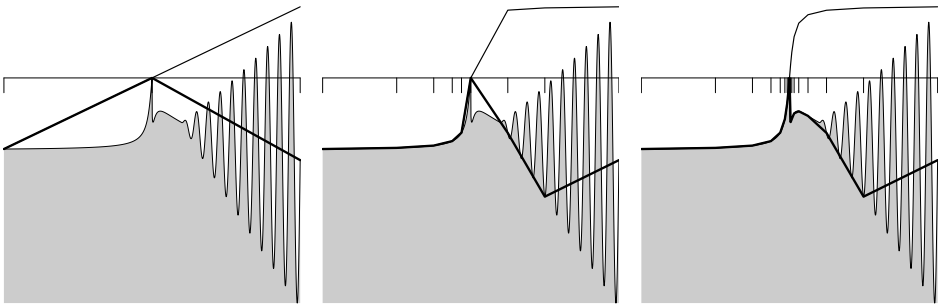

FIGURE 1.2. Localization for an oscillatory obstacle below u_h

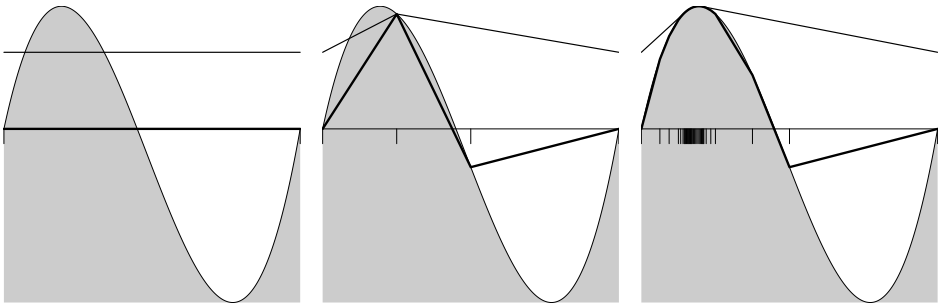

FIGURE 1.3. Localization for an obstacle not resolved on coarse grids

- It is not advisable to preadapt the mesh according to data f and χ since the contact set in unknown beforehand and its local mesh size should only depend on χ but not f, whereas the opposite situation occurs in the non-contact set.

Pointwise *a priori* error estimates for (1.1) were derived by Baiocchi [2] and Nitsche [10]. It is instructive to review briefly their approach since the present one is a "dual" version of it. To compare u with u_h, the Ritz projection $P_h u$ of u into the finite element space $\mathring{\mathbb{V}}_h$ is introduced, namely

$$P_h u \in \mathring{\mathbb{V}}_h : \quad \langle \nabla(u - P_h u), \nabla \varphi_h \rangle = 0 \quad \text{for all } \varphi_h \in \mathring{\mathbb{V}}_h.$$

Such $P_h u$ satisfies for *quasi-uniform* partitions $\mathcal{T}_h$ the following maximum norm error estimate [10], [14]:

$$\|u - P_h u\|_{0,\infty;\Omega} \leq \eta_1(u,h) = C_{\rm lin}\,|\log h|\,\omega(h), \tag{1.3}$$

where ω is the modulus of continuity of ∇u. If $\|\chi - \chi_h\|_{0,\infty;\Omega} \leq \eta_2(\chi,h)$, then

$$\|u - u_h\|_{0,\infty;\Omega} \leq C\big(\eta_1(u,h) + \eta_2(\chi,h)\big), \tag{1.4}$$

for a suitable constant C. The idea behind (1.4) is rather simple and elegant. The following functions $u_h^\pm$ are candidates for *discrete barriers*:

$$u_h^\pm := P_h u \pm C_{\rm bar}\big(\eta_1(u,h) + \eta_2(\chi,h)\big). \tag{1.5}$$

We then use the *discrete* maximum principle, which requires acute triangulations $\mathcal{T}_h$, to prove $u_h^- \leq u_h \leq u_h^+$. This, in conjunction with (1.3), results in (1.4).

To derive *a posteriori* error estimates we use a "dual approach". We start from the discrete solution u_h, instead of u, and modify it by adding a correction $w \in \mathring{H}^1(\Omega)$ which adjusts its Laplacian within elements and eliminates its jumps across inter-element sides. Such a w turns out to be the Riesz representation of a Galerkin functional closely related to that in [18], which for unconstrained problems reduces to the usual residual. We can thus estimate $\|w\|_{0,\infty;\Omega}$ by invoking improved variants of the results [4], [11] from linear theory. After suitable lifting of $u_h + w$, in the spirit of (1.5), the resulting function is a candidate for *continuous barrier* of (1.1). Application of the *continuous* maximum principle completes the argument without restrictions (as the acuteness in [2] and [10]) on the partition $\mathcal{T}_h$.

This paper is organized as follows. In §2 we introduce the discrete problem and discrete variables (u_h, σ_h), along with the positivity preserving operator Π_h of [3]. In §3 we discuss the Galerkin functional of [18], the localized residual and quadrature estimators, and their relation to the errors. We construct the continuous barriers in terms of the corrector w in §4, and derive pointwise estimates for w in §5. The upper a posteriori error estimates are proved in §5, whereas the corresponding lower bounds are shown in §6. We finally conclude in §7 with a number of simulations which clearly illustrate reliability, efficiency, and performance of the proposed estimators in 2d and 3d.

2. Discretization

Let $\{\mathcal{T}_h\}$ be a sequence of conforming partitions of $\overline{\Omega}$ into (closed) simplices. Given a simplex T, we write h_T for its diameter and ρ_T for the maximal radius of a ball that is contained in T. Shape-regularity of $\mathcal{T}_h$ is characterized by

$$\gamma(\mathcal{T}_h) := \max_{T\in\mathcal{T}_h} \frac{h_T}{\rho_T} \leq \gamma^*, \tag{2.1}$$

with γ^* bounded independently of h. In the sequel the same letter C will be used to denote different constants only depending on γ^*, the domain Ω, and the dimension d. In addition, we use $\preccurlyeq$ to indicate $\leq$ up to such constants C. The set of nodes of $\mathcal{T}_h$ is denoted by $\mathcal{N}_h$, and the subset of interior nodes by $\mathring{\mathcal{N}}_h$. The set of (closed) inter-element sides is denoted by $\mathcal{S}_h$.

Let $\mathbb{V}_h$ indicate the space of continuous piecewise linear finite element functions over $\mathcal{T}_h$ and $\mathring{\mathbb{V}}_h := \mathbb{V}_h \cap \mathring{H}^1(\Omega)$. The nodal basis functions of $\mathbb{V}_h$ are given by $(\phi_h^z)_{z\in\mathcal{N}_h}$. Let I_h be the Lagrange interpolation operator onto $\mathbb{V}_h$.

Given a subset ω of Ω, we let $\mathcal{U}_h(\omega)$ be a discrete neighborhood of ω, namely,

$$\mathcal{U}_h(\omega) := \bigcup \{T \in \mathcal{T}_h : T \cap \omega \neq \emptyset\}.$$

The star associated with a node $z \in \mathcal{N}_h$ is then $\mathcal{U}_h(z) := \mathcal{U}_h(\{z\}) = \operatorname{supp} \phi_z^h$.

2.1. **Discrete Problem.** Let $\chi_h := I_h \chi$ be the discrete obstacle and let $I_h g$ be the discrete Dirichlet datum. The discrete counterpart $\mathcal{K}_h$ of $\mathcal{K}$ is then

$$\mathcal{K}_h := \{v_h \in \mathbb{V}_h \mid v_h \geq \chi_h \text{ in } \Omega \text{ and } v_h = I_h g \text{ on } \partial\Omega\}.$$

The set $\mathcal{K}_h$ is non-empty, convex, closed but in general not a subset of $\mathcal{K}$ (non-conforming approximation). Given the scalar products

$$\langle \varphi, \psi \rangle = \int_\Omega \varphi\psi, \qquad \langle\langle \varphi, \psi \rangle\rangle = \int_{\partial\Omega} \varphi\psi,$$

the *discrete problem* reads as follows:

$$u_h \in \mathcal{K}_h : \quad \langle \nabla u_h, \nabla(u_h - v_h) \rangle \leq \langle f, u_h - v_h \rangle \qquad \text{for all } v_h \in \mathcal{K}_h. \tag{2.2}$$

Problem (2.2) admits a unique solution (use [8], [9] in the Hilbert space $\mathbb{V}_h$).

We denote by $\langle \cdot, \cdot \rangle_h$ the lumped L_2 scalar product, i. e.,

$$\langle \varphi_h, \psi_h \rangle_h := \int_\Omega I_h(\varphi_h \psi_h) \qquad \text{for all } \varphi_h, \psi_h \in \mathbb{V}_h.$$

We next introduce the discrete approximation $\sigma_h \in \mathbb{V}_h$ to the measure σ. For interior nodes $z \in \mathring{\mathcal{N}}_h$, we set

$$\langle \sigma_h, \phi_h^z \rangle_h = \langle f, \phi_h^z \rangle - \langle \nabla u_h, \nabla \phi_h^z \rangle,$$

whence

$$\sigma_h(z) = \left(\textstyle\int_\Omega \phi_h^z\right)^{-1} \left(\langle f, \phi_h^z \rangle - \langle \nabla u_h, \nabla \phi_h^z \rangle \right),$$

and $\sigma_h(z) \leq 0$. Inspired by this expression, we extend the definition of $\sigma_h(z)$ to boundary nodes z as follows:

$$\sigma_h(z) = \begin{cases} -\dfrac{\left(\langle f, \phi_h^z \rangle - \langle \nabla u_h, \nabla \phi_h^z \rangle + \langle\langle \partial_n u_h, \phi_h^z \rangle\rangle \right)^-}{\int_\Omega \phi_h^z}, & \text{if } \mathcal{U}_h(z) \subset \{u_h = \chi_h\}, \\ 0, & \text{otherwise.} \end{cases}$$

Hereafter, n denotes the outer normal of Ω and $v^- := -\min\{v, 0\}$ is the negative part of a function v. We conclude that $\sigma_h \leq 0$ in $\bar{\Omega}$.

We finally split the triangulation $\mathcal{T}_h$ into

$$\mathcal{T}_h^0 := \left\{T \in \mathcal{T}_h \mid \mathcal{U}_h(T) \subset \{u_h - \chi_h = 0\}\right\}, \qquad \mathcal{T}_h^+ := \mathcal{T}_h \backslash \mathcal{T}_h^0, \tag{2.3}$$

and Ω into *discrete contact set* Λ_h and *discrete non-contact set* $\Omega \backslash \Lambda_h$ with

$$\Lambda_h := \bigcup \{T : T \in \mathcal{T}_h^0\}. \tag{2.4}$$

2.2. **Positivity Preserving Interpolation.** We call a linear interpolation operator $\Pi_h\colon L_1(\Omega) \to \mathring{\mathbb{V}}_h$ *positive* if

$$\varphi \geq 0 \quad \Rightarrow \quad \Pi_h \varphi \geq 0. \tag{2.5}$$

Since we will make extensive use of the operator introduced by Chen and Nochetto [3], we recall its definition. Given $z \in \mathring{\mathcal{N}}_h$ and $\varphi \in L_1(\Omega)$, we choose $B(z)$ to be a ball contained in the star $\mathcal{U}_h(z)$ and define the nodal value

$$\Pi_h \varphi(z) := \frac{1}{|B(z)|} \int_{B(z)} \varphi. \tag{2.6}$$

The radius of $B(z)$ must be comparable with the local mesh size for Π_h to possess the desired properties (listed below) uniformly in the mesh size. In Section 6 we will investigate a suitable choice of radius.

It is clear from (2.6) that Π_h satisfies (2.5). The following properties are valid for all $1 \leq p \leq \infty$, $T \in \mathcal{T}_h$ and $S \in \mathcal{S}_h$ [3]:

$$\|\nabla \Pi_h \varphi\|_{0,p;T} \preccurlyeq \|\nabla \varphi\|_{0,p;\mathcal{U}_h(T)}, \tag{2.7a}$$

$$\|\varphi - \Pi_h \varphi\|_{0,p;T} \preccurlyeq h_T \|\nabla \varphi\|_{0,p;\mathcal{U}_h(T)}, \tag{2.7b}$$

$$\|\varphi - \Pi_h \varphi\|_{0,p;S} \preccurlyeq h_S^{1-1/p} \|\nabla \varphi\|_{0,p;\mathcal{U}_h(S)}, \tag{2.7c}$$

provided $\varphi \in \mathring{W}^1_p(\Omega)$. For $\varphi \in \mathring{W}^1_1(\Omega)$ with $\nabla \varphi \in BV(\Omega)^d$, we also have

$$\|\varphi - \Pi_h \varphi\|_{0,1;T} \preccurlyeq h_T^2 |D^2 \varphi|_{\mathrm{var}}\big(\mathcal{U}_h(T)\big), \tag{2.7d}$$

$$\|\varphi - \Pi_h \varphi\|_{0,1;S} \preccurlyeq h_S |D^2 \varphi|_{\mathrm{var}}\big(\mathcal{U}_h(S)\big), \tag{2.7e}$$

where

$$|D^2 \varphi|_{\mathrm{var}} := \sum_{i=1}^{d} |D \partial_i \varphi|_{\mathrm{var}} \tag{2.8}$$

is the sum of the variation measures $|D\partial_i \varphi|_{\mathrm{var}}$ of $\partial_i \varphi$, $i = 1, \ldots, d$; see e. g. [6, Section 5.1]. Note that, if $\varphi \in W^2_1(\Omega)$ and ω is a measurable subset of Ω, then $|D^2 \varphi|_{\mathrm{var}}(\omega) = \|D^2 \varphi\|_{0,1;\omega}$. Estimate (2.7d) follows from local stability of Π_h in L_1, validity of a similar estimate in W^2_1, and approximation of φ by smooth functions φ_k such that $\varphi_k, \nabla \varphi_k \to \varphi, \nabla \varphi$ in $L_1(\mathcal{U}_h(T))$ and $\|D^2 \varphi_k\|_{0,1;\mathcal{U}_h(T)} \to |D^2 \varphi|_{\mathrm{var}}\big(\mathcal{U}_h(T)\big)$ as $k \to \infty$ (cf. Theorem 2 in [6, Section 5.2]). Similarly, one obtains (2.7e).

Note that Π_h is not a projection operator, namely $\Pi_h^2 \neq \Pi_h$, and that the case of homogeneous boundary values is special for linear positive finite element interpolation operators; see Nochetto and Wahlbin [12].

3. Error and Estimators

Our error concept involves not only the pointwise error $u - u_h$ but also an error associated to the measure σ. We will not compare σ with σ_h, but rather with the following quantity $\tilde{\sigma}_h \in L_2(\Omega)$ defined by

$$\langle \tilde{\sigma}_h, \varphi \rangle = \sum_{T \in \mathcal{T}_h^0} \int_T \sigma_h \, \varphi + \sum_{T \in \mathcal{T}_h^+} \int_T I_h(\sigma_h \, \Pi_h \varphi) \qquad \text{for all } \varphi \in L_2(\Omega) \tag{3.1}$$

with $\mathcal{T}_h^0$ and $\mathcal{T}_h^+$ as in (2.3). Such $\tilde{\sigma}_h$ exhibits more suitable cancellation and localization properties than σ_h in connection with the pointwise error $u - u_h$. We point out that $\tilde{\sigma}_h$ is not piecewise linear, but like σ_h it does satisfy

$$\tilde{\sigma}_h \leq 0 \tag{3.2}$$

because of (2.5). Moreover, $\tilde{\sigma}_h$ is only needed in the subsequent analysis but not in the estimator. We finally note that, in light of (2.6), $\tilde{\sigma}_h|_T = \sigma_h|_T$ for all $T \in \mathcal{T}_h^0$ such that $\mathcal{U}_h(T) \subset \Lambda_h$ as well as those T for which $\mathcal{U}_h(T) \subset \{\sigma_h = 0\}$.

3.1. **Galerkin Functional.** We are now in the position to define the Galerkin functional $\mathcal{G}_h \in H^{-1}(\Omega)$, which plays the role of the residual for (unconstrained) equations:

$$\begin{aligned} \langle \mathcal{G}_h,\, \varphi\rangle &:= \langle \nabla(u-u_h),\, \nabla\varphi\rangle + \langle \sigma - \tilde{\sigma}_h,\, \varphi\rangle \\ &= -\langle \nabla u_h,\, \nabla\varphi\rangle + \langle f - \tilde{\sigma}_h,\, \varphi\rangle \qquad \text{for all } \varphi \in \mathring{H}^1(\Omega). \end{aligned} \tag{3.3}$$

Note that this definition of the Galerkin functional $\mathcal{G}_h$ differs slightly from the one in Veeser [18]. In fact, we have $\tilde{\sigma}_h$ instead of σ_h in (3.3).

Our next task is to investigate properties of $\mathcal{G}_h$ and relate $\mathcal{G}_h$ to the errors. We first observe that $\mathcal{G}_h$ satisfies the *almost Galerkin orthogonality* property

$$\begin{aligned} \langle \mathcal{G}_h,\, \varphi_h\rangle &= \langle \sigma_h,\, \varphi_h\rangle_h - \langle \tilde{\sigma}_h,\, \varphi_h\rangle \\ &= \sum_{T\in\mathcal{T}_h^0} \int_T I_h(\sigma_h\,\varphi_h) - \sigma_h\,\varphi_h \;+\; \sum_{T\in\mathcal{T}_h^+} \int_T I_h\big(\sigma_h\,(\varphi_h - \Pi_h\varphi_h)\big), \end{aligned} \tag{3.4}$$

for all $\varphi_h \in \mathring{\mathbb{V}}_h$. Making use of (3.4), we can write for any $\varphi \in H_0^1(\Omega)$

$$\begin{aligned} \langle \mathcal{G}_h,\, \varphi\rangle &= \langle \mathcal{G}_h,\, \varphi - \Pi_h\varphi\rangle + \langle \mathcal{G}_h,\, \Pi_h\varphi\rangle \\ &= \sum_{S\in\mathcal{S}_h} \int_S [\![\partial_\nu u_h]\!]\,(\varphi - \Pi_h\varphi) \;+\; \sum_{T\in\mathcal{T}_h^0} \int_T (f-\sigma_h)\,(\varphi - \Pi_h\varphi) \\ &\quad + \sum_{T\in\mathcal{T}_h^+} \int_T f\,(\varphi - \Pi_h\varphi) - I_h\big(\sigma_h\,(\Pi_h\varphi - \Pi_h^2\varphi)\big) \\ &\quad + \sum_{T\in\mathcal{T}_h^0} \int_T I_h(\sigma_h\,\Pi_h\varphi) - \sigma_h\,\Pi_h\varphi \;+\; \sum_{T\in\mathcal{T}_h^+} \int_T I_h\big(\sigma_h\,(\Pi_h\varphi - \Pi_h^2\varphi)\big), \end{aligned}$$

where $[\![\partial_\nu u_h]\!]$ is the jump across sides S in the normal derivative of u_h; recall that $\Pi_h^2 \neq \Pi_h$. Here, one can see the cancellations built in the definition of $\tilde{\sigma}_h$. The cancellation $f - \sigma_h$ over $\mathcal{T}_h^0$ is responsible for *localization* in our error estimators, while the cancellation of $I_h\big(\sigma_h\,(\Pi_h^2\varphi - \Pi_h\varphi)\big)$ over $\mathcal{T}_h^+$ is the reason for dealing with $\tilde{\sigma}_h$ instead of σ_h (see (3.6) and (3.12) below). Thus, defining $\mathcal{R}_h \in H^{-1}(\Omega)$ by

$$\langle \mathcal{R}_h,\, \varphi\rangle := \sum_{S\in\mathcal{S}_h} \int_S [\![\partial_\nu u_h]\!]\,\varphi \;+\; \sum_{T\in\mathcal{T}_h^0} \int_T (f-\sigma_h)\,\varphi \;+\; \sum_{T\in\mathcal{T}_h^+} \int_T f\,\varphi$$

and $\mathcal{Q}_h \in \mathring{\mathbb{V}}_h$ by

$$\langle \mathcal{Q}_h,\, \varphi_h\rangle := \sum_{T\in\mathcal{T}_h^0} \int_T I_h(\sigma_h\,\varphi_h) - \sigma_h\,\varphi_h,$$

we have the following representation formula for $\mathcal{G}_h$:

$$\langle \mathcal{G}_h,\, \varphi\rangle = \langle \mathcal{R}_h,\, \varphi - \Pi_h\varphi\rangle + \langle \mathcal{Q}_h,\, \Pi_h\varphi\rangle\,. \tag{3.5}$$

In contrast to (3.5), using σ_h instead of $\tilde{\sigma}_h$ in (3.3), as in [18], would have led to

$$\begin{aligned} \langle \mathcal{G}_h,\, \varphi\rangle = &\sum_{S\in\mathcal{S}_h} \int_S [\![\partial_\nu u_h]\!]\,(\varphi - \Pi_h\varphi) \;+\; \sum_{T\in\mathcal{T}_h} \int_T (f-\sigma_h)\,(\varphi - \Pi_h\varphi) \\ &+\; \big[\langle \sigma_h,\, \Pi_h\varphi\rangle_h - \langle \sigma_h,\, \Pi_h\varphi\rangle\big]. \end{aligned} \tag{3.6}$$

This alternative representation formula does not yield a second order estimator and is further discussed in (3.12). This justifies the use of $\tilde{\sigma}_h$ and Π_h.

3.2. **Localized Residual and Quadrature Estimators.** The estimation of the pointwise error $\|u-u_h\|_{0,\infty;\Omega}$ can be reduced to an appropriate control of $\mathcal{G}_h$. This crucial step will be performed in §4 and will require an estimate for $\mathcal{G}_h$ in the dual space of $W_1^2(\Omega)\cap\mathring{H}^1(\Omega)$. We now simply derive an estimate for $\mathcal{G}_h$ in the dual space W^* of

$$W := \{\varphi\in\mathring{H}^1(\Omega)\mid \nabla\varphi\in BV(\Omega)^d\}$$

equipped with the norm $\varphi\mapsto|D^2\varphi|_{\mathrm{var}}(\Omega)$ (see (2.8)). The space W is slightly bigger than $W_1^2(\Omega)\cap\mathring{H}^1(\Omega)$ and contains the discrete space $\mathring{\mathbb{V}}_h$. This fact will be useful for the discussion in §6.3. The estimate for $\mathcal{G}_h$ leads to residual type and quadrature estimators.

We define the *localized residual* R_p over $T\in\mathcal{T}_h$ for any $1\le p\le\infty$ to be

$$R_p|_T = h_T^{-1/p'}|T|^{-1/p}\|\,[\![\partial_\nu u_h]\!]\,\|_{0,p;\partial T\setminus\partial\Omega} + \begin{cases}|f-\sigma_h| & T\in\mathcal{T}_h^0\\ |f| & T\in\mathcal{T}_h^+,\end{cases} \tag{3.7}$$

where $p'=p/(p-1)$ is the dual exponent of p. In light of (2.7d), (2.7e), and the additivity of $|D^2\varphi|_{\mathrm{var}}$, the localized residual bounds $\langle\mathcal{R}_h,\,\varphi-\Pi_h\varphi\rangle$ as follows:

$$|\langle\mathcal{R}_h,\,\varphi-\Pi_h\varphi\rangle| \preccurlyeq \|h^2R_\infty\|_{0,\infty;\Omega}\,|D^2\varphi|_{\mathrm{var}}(\Omega). \tag{3.8}$$

The second term $\langle\mathcal{Q}_h,\,\Pi_h\varphi\rangle$ on the right-hand side of (3.5) accounts for the effect of quadrature; this contribution occurs also for unconstrained linear problems with quadrature. The Bramble-Hilbert lemma, (2.7a), and the Sobolev-type inequality $\|\nabla\varphi\|_{0,d';\Omega}\preccurlyeq|D^2\varphi|_{\mathrm{var}}(\Omega)$ for $\varphi\in W$ imply

$$\begin{aligned}|\langle\mathcal{Q}_h,\,\Pi_h\varphi\rangle| &\preccurlyeq \|h^2\nabla\sigma_h\|_{0,d;\Lambda_h}\,\|\nabla\Pi_h\varphi\|_{0,d';\Omega}\\ &\preccurlyeq \|h^2\nabla\sigma_h\|_{0,d;\Lambda_h}|D^2\varphi|_{\mathrm{var}}(\Omega).\end{aligned} \tag{3.9}$$

Inserting (3.8) and (3.9) into the (3.5), we deduce the upper bound

$$\|\mathcal{G}_h\|_{-2,\infty;\Omega}\preccurlyeq\|h^2R_\infty\|_{0,\infty;\Omega}+\|h^2\nabla\sigma_h\|_{0,d;\Lambda_h}, \tag{3.10}$$

where

$$\|\mathcal{G}_h\|_{-2,\infty;\Omega} := \sup\big\{\langle\mathcal{G}_h,\,\varphi\rangle\mid\varphi\in W\text{ with }|D^2\varphi|_{\mathrm{var}}(\Omega)\le1\big\}.$$

The actual estimators $\mathcal{E}_h$, to be discussed in §5, contain not only the terms on the right-hand side of (3.10) but also additional consistency terms. We will show that

$$\|u-u_h\|_{0,\infty;\Omega}\preccurlyeq\mathcal{E}_h.$$

Combined with (3.3) and

$$\int_\Omega\nabla(u-u_h)\cdot\nabla\varphi\le\|u-u_h\|_{0,\infty;\Omega}\,|D^2\varphi|_{\mathrm{var}}(\Omega)$$

for all $\varphi\in W$ (approximate $u-u_h$ appropriately), this leads to

$$\|\sigma-\tilde{\sigma}_h\|_{-2,\infty;\Omega}\preccurlyeq\mathcal{E}_h.$$

It is crucial to see that, invoking (3.3) once again, we easily obtain the lower bound

$$\|\mathcal{G}_h\|_{-2,\infty;\Omega}\le\|u-u_h\|_{0,\infty;\Omega}+\|\sigma-\tilde{\sigma}_h\|_{-2,\infty;\Omega}. \tag{3.11}$$

These estimates, similar to those in [18, Lemma 3.4], explain why the Galerkin functional $\mathcal{G}_h$ is intimately related to the error in both u and σ and that, except

possibly for consistency terms, it contains the correct information about the problem at hand. In the next two sections, we elaborate further on this issue.

Before we do so, note that the term between the square brackets in (3.6) would yield the following expression for (3.9):

$$|\langle \mathcal{Q}_h, \Pi_h\varphi\rangle| \preccurlyeq \|h^2\nabla\sigma_h\|_{0,d;\Omega}\, |D^2\varphi|_{\mathrm{var}}(\Omega). \tag{3.12}$$

Since σ_h changes rapidly across the boundary of Λ_h, this term does not exhibit the desired asymptotic second order, and thus spoils the overall error estimation.

4. Upper Bound I: Barriers

Let w be the Riesz representation in $\mathring{H}^1(\Omega)$ of the Galerkin functional $\mathcal{G}_h$, i. e.

$$w \in \mathring{H}^1(\Omega): \qquad \int_\Omega \nabla w\cdot\nabla\varphi = \langle \mathcal{G}_h,\, \varphi\rangle \quad \text{for all } \varphi\in\mathring{H}^1(\Omega). \tag{4.1}$$

With the help of w we construct now upper and lower barriers of u that involve, besides w, only computable quantities which account for consistency errors. We thereby suppose that w is continuous – a fact that is proven in the next section.

4.1. **Upper Barrier.** Let $v^+ = \max\{v, 0\}$ denote the non-negative part of a function v. We now construct a (continuous) upper barrier u^* of u.

Proposition 4.1 (Upper barrier)**.** *The function*

$$u^* := u_h + w + \|w\|_{0,\infty;\Omega} + \|g - I_h g\|_{0,\infty;\partial\Omega} + \|(\chi - u_h)^+\|_{0,\infty;\Omega} \tag{4.2}$$

satisfies

$$u \le u^* \qquad \text{in } \Omega.$$

Proof. **1.** Since

$$(u-u^*)_{|\partial\Omega} \;\le\; (u-u_h)_{|\partial\Omega} - \|g - I_h g\|_{0,\infty;\partial\Omega} \;\le\; 0,$$

the function $v := (u-u^*)^+$ satisfies

$$v_{|\partial\Omega} = 0. \tag{4.3}$$

We want to show that $\|\nabla v\|_{2;\Omega} = 0$ and then use (4.3) to conclude that $v = 0$.

2. In view of (3.1) and (3.3), we can write

$$\begin{aligned} \|\nabla v\|^2_{0,2;\Omega} &= \int_\Omega \nabla(u-u^*)\cdot\nabla v = \int_\Omega \nabla(u-u_h)\cdot\nabla v - \int_\Omega \nabla w\cdot\nabla v \\ &= \langle \tilde\sigma_h - \sigma,\, v\rangle \le -\langle \sigma,\, v\rangle\,. \end{aligned} \tag{4.4}$$

It thus remains to show that $\langle \sigma, v\rangle = 0$.

3. Since σ is a Radon measure (see e. g. [9, Theorem 6.9]) and v continuous, we may write

$$\langle \sigma, v\rangle = \int_\Omega v\, d\sigma. \tag{4.5}$$

We recall that the support of σ is in the closed contact set $\{u = \chi\}$, or equivalently

$$\int_\Omega \varphi\, d\sigma = 0 \quad \text{for all } \varphi\in C_0^0(\{u>\chi\}).$$

On the other hand, we have $\{v>0\} = \{u>u^*\} \subset \{u>\chi\}$ because

$$u \;>\; u^* \;\ge\; \chi - (\chi - u_h) + \|(\chi-u_h)^+\|_{0,\infty;\Omega} \;\ge\; \chi.$$

A partition of unity of the open set $\{u > \chi\}$ thus allows us to reduce the pairing (4.5) to functions v with compact support contained in $\{u > \chi\}$ and for which the result is zero. □

4.2. **Lower Barrier.** We now construct a (continuous) lower barrier u_* of u.

Proposition 4.2 (Lower barrier). *The function*

$$u_* := u_h + w - \|w\|_{0,\infty;\Omega} - \|g - I_h g\|_{0,\infty;\partial\Omega} - \|(u_h - \chi)^+\|_{0,\infty;\{\sigma_h<0\}} \tag{4.6}$$

satisfies

$$u_* \le u \qquad \text{in } \Omega.$$

Proof. **1.** Arguing as in steps 1 and 2 of Proposition 4.1, it suffices to prove

$$\langle \tilde{\sigma}_h,\, v\rangle = 0 \tag{4.7}$$

for the function $v := (u_* - u)^+$.

2. Before establishing (4.7), we show the important property:

$$\text{If there exists } x \in \operatorname{int}(T) \text{ such that } u_*(x) > u(x), \text{ then } \sigma_{h|T} = 0.$$

Let $u_*(x) > u(x)$ for some $x \in \operatorname{int}(T)$. If we had $\sigma_h(x) < 0$, then (4.6) would imply

$$u_h(x) > \chi(x) + \|(u_h - \chi)^+\|_{0,\infty;\{\sigma_h<0\}} \ge u_h(x),$$

a contraction; hence $\sigma_h(x) = 0$. Since $\sigma_h \le 0$ is affine in T, we arrive at $\sigma_{h|T} = 0$.

3. Invoking the definition (3.1) of $\tilde{\sigma}_h$, namely,

$$\langle \tilde{\sigma}_h,\, v\rangle = \sum_{T\in\mathcal{T}_h^0} \int_T \sigma_h\, v + \sum_{T\in\mathcal{T}_h^+} \int_T I_h(\sigma_h\, \Pi_h v)$$

we have to show that for each $T \in \mathcal{T}_h$ the corresponding integral vanishes.

Let $T \in \mathcal{T}_h^0$. If $v = 0$ in T, then $\int_T \sigma_h v = 0$. Otherwise, there exists an $x \in \operatorname{int}(T)$ with $v(x) > 0$ and we obtain $\int_T \sigma_h v = 0$ by step 2.

Let $T \in \mathcal{T}_h^+$. We may write

$$\int_T I_h(\sigma_h\, \Pi_h v) = \frac{|T|}{d+1} \sum_{i=0}^{d} \sigma_h(z_i)(\Pi_h v)(z_i),$$

where $z_0, \dots, z_d$ are the vertices of simplex T. For boundary nodes z_i, there is no contribution on the right hand side, because $\Pi_h v = 0$ on $\partial\Omega$. For an interior vertex z_i with $(\Pi_h v)(z_i) > 0$, we get from (2.6) that $v(x) > 0$ for some $x \in \mathcal{U}_h(z_i)$. Step 2 thus implies $\sigma_h(z_i) = 0$, and (4.7) follows, thereby proving the assertion. □

Remark 4.3 (Optimal choice). In (4.6) and the proof of Proposition 4.2, it would suffice to deal with $\|(u_h - u)^+\|_{0,\infty;\{\sigma_h<0\}}$ instead of $\|(u_h - \chi)^+\|_{0,\infty;\{\sigma_h<0\}}$. This would indeed be an optimal, but *non-computable*, choice.

4.3. **Partial Pointwise Error Estimate.** Propositions 4.1 and 4.2 yield

$$\begin{aligned} \|u - u_h\|_{0,\infty;\Omega} \le\ & 2\,\|w\|_{0,\infty;\Omega} + \|g - I_h g\|_{0,\infty;\partial\Omega} \\ & + \|(\chi - u_h)^+\|_{0,\infty;\Omega} + \|(u_h - \chi)^+\|_{0,\infty;\{\sigma_h<0\}}. \end{aligned} \tag{4.8}$$

Besides $\|w\|_{0,\infty;\Omega}$, all terms involve only given data and the discrete solution and are computable. It remains to estimate $\|w\|_{0,\infty;\Omega}$ in terms of computable quantities. This is a question about the *linear* problem (4.1), and is carried out in §5.

5. Upper Bound II: Pointwise Estimates

In this section we derive pointwise estimates for both w and the error $u - u_h$.

5.1. **Pointwise Estimates of w.** In order to obtain a pointwise estimate for $w = (-\Delta)^{-1}\mathcal{G}_h$ we proceed in three steps. We first bound w in a Hölder space, thus stronger than $L_\infty(\Omega)$. We then give an estimate weaker than $\|w\|_{0,\infty;\Omega}$, and finally we combine these two estimates.

In the previous section we used the continuity of w. This property is derived in the next lemma.

Lemma 5.1 (Hölder continuity of w and its control)**.** *The Riesz representation w of the Galerkin functional $\mathcal{G}_h$ is Hölder continuous. More precisely, for every $p > d$ there exists $\alpha \in (0,1)$ such that*

$$\|w\|_{C^{0,\alpha}(\Omega)} \preccurlyeq \left(\|hR_p\|_{0,p;\Omega} + \|h^2\nabla\sigma_h\|_{0,p;\Lambda_h}\right), \tag{5.1}$$

where the constant hidden in $\preccurlyeq$ depends on Ω and p, and blows up as $p \downarrow d$.

Proof. Let $p' = p/(p-1)$ be the dual exponent of $p > d$. A classical Hölder estimate of De Giorgi and Nash reads

$$\|w\|_{C^{0,\alpha}(\Omega)} \preccurlyeq \|\mathcal{G}_h\|_{-1,p;\Omega} = \sup\{\langle \mathcal{G}_h,\, \varphi\rangle \mid \varphi \in \mathring{W}^{1,p'}(\Omega),\ \|\nabla\varphi\|_{0,p';\Omega} \le 1\},$$

where the latter is the norm in the dual space of $\mathring{W}^{1,p'}(\Omega)$ (see e. g. [9, Theorem C.2]); the constant hidden in $\preccurlyeq$ depends on Ω and p, and blows up as $p \downarrow d$. In view of (3.5), we can estimate

$$\langle \mathcal{G}_h,\, \varphi\rangle \preccurlyeq \left(\|hR_p\|_{0,p;\Omega} + \|h^2\nabla\sigma_h\|_{0,p;\Lambda_h}\right)^{1/p} \|\nabla\varphi\|_{0,p';\Omega} \quad \text{for all } \varphi \in \mathring{W}^{1,p'}(\Omega),$$

where we have used the Bramble-Hilbert lemma and (2.7). This proves (5.1). □

Note that the right-hand side of (5.1) is a *first order* estimator, while we have to estimate $\|w\|_{0,\infty;\Omega}$ by a *second order* estimator. A key step is performed next.

Since w is continuous and satisfies $w_{|\partial\Omega} = 0$, there exists a $x_0 \in \Omega$ with $|w(x_0)| = \|w\|_{0,\infty;\Omega}$. Invoking the uniform cone property of Ω [1, Section 4.7], we can choose a ball B with radius ρ such that $B \subset \Omega$, $\operatorname{dist}(x_0, B) \preccurlyeq \rho$, and $\rho = Ch_{\min}^\beta$, where $\beta > 1$ will be chosen later. Let $\delta \in C_0^\infty(\Omega)$ be a regularization of the Dirac mass satisfying

$$\operatorname{supp}\delta \subset B, \qquad \int_\Omega \delta = 1, \qquad 0 \le \delta \preccurlyeq \rho^{-d}. \tag{5.2}$$

Taking $x_1 \in B$ such that $\langle \delta,\, w\rangle = w(x_1)$, we may write

$$\|w\|_{0,\infty;\Omega} \le |\langle \delta,\, w\rangle| + |w(x_0) - w(x_1)|. \tag{5.3}$$

Lemma 5.1 implies the following estimate for the second term of (5.3):

$$|w(x_0) - w(x_1)| \preccurlyeq h_{\min}^{\alpha\beta}\left(\|hR_p\|_{0,p;\Omega} + \|h^2\nabla\sigma_h\|_{0,p;\Lambda_h}\right). \tag{5.4}$$

In order to bound the first term of (5.3), we introduce the regularized Green's function $G \in \mathring{H}^1(\Omega)$ defined by

$$\langle \nabla G,\, \nabla\varphi\rangle = \langle \delta,\, \varphi\rangle \qquad \text{for all } \varphi \in \mathring{H}^1(\Omega).$$

The following a priori estimate has been proved by Nochetto [11] in 2d and Dari *et al.* [4] in 3d for any polyhedral domain Ω:

$$\|D^2 G\|_{0,1;\Omega} + \|DG\|_{0,d/(d-1);\Omega} \preccurlyeq |\log h_{\min}|^2, \tag{5.5}$$

where the constant hidden in $\preccurlyeq$ depends on β via ρ. This result is instrumental to prove the following bound.

Lemma 5.2 (Estimate of $\langle \delta, w \rangle$). *The regularized Dirac mass δ of* (5.2) *and the Riesz representation w of* (4.1) *satisfy*

$$|\langle \delta, w \rangle| \;\preccurlyeq\; |\log h_{\min}|^2 \Big(\|h^2 R_\infty\|_{0,\infty;\Omega} + \|h^2 \nabla \sigma_h\|_{0,d;\Lambda_h} \Big).$$

where the geometric constant hidden in $\preccurlyeq$ depends on β via ρ.

Proof. In light of (3.8), (3.9), and (5.5), we obtain

$$\begin{aligned} \langle \delta, w \rangle = \langle \nabla G, \nabla w \rangle = \langle \mathcal{G}_h, G \rangle &= \langle \mathcal{R}_h, G - \Pi_h G \rangle + \langle \mathcal{Q}_h, \Pi_h G \rangle \\ &\preccurlyeq \|h^2 R_\infty\|_{0,\infty;\Omega} \|D^2 G\|_{0,1;\Omega} + \|h^2 \nabla \sigma_h\|_{0,d;\Lambda_h} \|DG\|_{0,d/(d-1);\Omega} \\ &\preccurlyeq |\log h_{\min}|^2 \Big(\|h^2 R_\infty\|_{0,\infty;\Omega} + \|h^2 \nabla \sigma_h\|_{0,d;\Lambda_h} \Big), \end{aligned}$$

as desired. □

Combining the two previous lemmas yields the main result of this section.

Proposition 5.3 (Pointwise estimate of $|w|$). *The maximum norm of the Riesz representation w of the Galerkin functional $\mathcal{G}_h$ satisfies the a posteriori bound*

$$\|w\|_{0,\infty;\Omega} \;\preccurlyeq\; |\log h_{\min}|^2 \Big(\|h^2 R_\infty\|_{0,\infty;\Omega} + \|h^2 \nabla \sigma_h\|_{0,d;\Lambda_h} \Big) \tag{5.6}$$

Proof. For $p > d$ fixed and $\beta = 1/\alpha$, we see that $h_{\min}^{\alpha\beta} \le h_T \le C$ for all $T \in \mathcal{T}_h$, and thereby the right-hand side of (5.4) satisfies

$$h_{\min}^{\alpha\beta} \left(\|h R_p\|_{0,p;\Omega} + \|h^2 \nabla \sigma_h\|_{0,p;\Lambda_h} \right) \preccurlyeq \|h^2 R_\infty\|_{0,\infty;\Omega} + \|h^2 \nabla \sigma_h\|_{0,d;\Lambda_h}.$$

The last term results from $(\sum_T a_T^p)^{1/p} \le (\sum_T a_T^d)^{1/d}$ for $a_T = h_T^{2+d/p} |\nabla \sigma_h|_T|$. Consequently, the assertion follows by combining (5.4) and Lemma 5.2. □

5.2. **Pointwise Upper Bound.** We now collect the results of §4.3 and §5.1. Let C_0 and C_1 be twice the constants hidden in (5.6). The pointwise estimator $\mathcal{E}_h$ is

$$\begin{aligned} \mathcal{E}_h := {} & C_0 |\log h_{\min}|^2 \; \|h^2 R_\infty\|_{0,\infty;\Omega} && \textit{localized residual} \\ & + C_1 |\log h_{\min}|^2 \; \|h^2 \nabla \sigma_h\|_{0,d;\Lambda_h} && \textit{localized quadrature} \\ & + \|(\chi - u_h)^+\|_{0,\infty;\Omega} + \|(u_h - \chi)^+\|_{0,\infty;\{\sigma_h < 0\}} && \textit{localized obstacle approx.} \\ & + \|g - I_h g\|_{0,\infty;\partial\Omega}. && \textit{boundary datum approx.} \end{aligned}$$

Theorem 5.4 (Reliability). *Let (u, σ) satisfy* (1.1) *and* (1.2), *as well as $(u_h, \tilde{\sigma}_h)$ satisfy* (2.2) *and* (3.1). *Then the following a posteriori error estimate holds*

$$\max \Big\{ \|u - u_h\|_{0,\infty;\Omega}, \; \|\sigma - \tilde{\sigma}_h\|_{-2,\infty;\Omega} \Big\} \le \mathcal{E}_h. \tag{5.7}$$

Proof. This is an immediate consequence of (4.8) and (5.6). □

Several remarks are now in order about the various terms in (5.7), their optimal character, and their connection to Figures 1.1-1.3.

Remark 5.5 (Improvement of [4], [11]). Lemma 5.1 applies also in the linear case (without obstacle), and improves upon the assumption $h_{\min} \ge h_{\max}^\gamma$ with $\gamma > 1$.

Remark 5.6 (Mesh grading in Λ_h)**.** For piecewise linear obstacles χ, the mesh size within the discrete contact set might not tend to zero because all terms in $\mathcal{E}_h$ could vanish there. This happens in Figure 1.1 and Example 7.2, and shows that the assumption $h_{\min} \geq h_{\max}^{\gamma}$ with $\gamma > 1$ of [4], [11] may be inadequate in this case.

Remark 5.7 (Localization of the interior residual)**.** In view of (3.7) and (5.7), the interior residual in the discrete contact set Λ_h reads

$$\|h^2(f - \sigma_h)\|_{0,\infty;\Lambda_h}.$$

The presence of σ_h is responsible for coarse meshes within Λ_h, irrespective of the magnitude of f, for as long as u is smooth. This is the case of Figures 1.1-1.2.

Remark 5.8 (Role of $\|(u_h - \chi)^+\|_{0,\infty;\{\sigma_h<0\}}$)**.** Notice that for the leftmost picture in Figure 1.1 we have $u_h = \chi_h$, whence $\sigma_h = f = -1$ and $\Lambda_h = \Omega$. Since u_h is also flat, then all estimators in (5.7) vanish except for $\|(u_h - \chi)^+\|_{0,\infty;\{\sigma_h<0\}}$, which drives the refinement initially. Once u_h detaches from χ_h, then $\sigma_h = 0$ and thus $\|(u_h - \chi)^+\|_{0,\infty;\{\sigma_h<0\}}$ does no longer force refinement near the downward cusp of Figure 1.1 thereby avoiding over-refinement; see middle and rightmost pictures of Figure 1.1. The same localization effect takes place in Figure 1.2 because the oscillatory part of obstacle χ is below u_h and thus $\sigma_h = 0$. The mesh is coarse, thus reflecting the structure of u, and not that of χ.

Remark 5.9 (Role of $\|(\chi - u_h)^+\|_{0,\infty;\Omega}$)**.** Consider Figure 1.3 which was obtained with load function $f = 0$. Since u_h is constant in the leftmost picture, σ_h vanishes. We thus see that all estimators are zero except for $\|(\chi - u_h)^+\|_{0,\infty;\Omega}$, which drives the initial refinement; this term detects $u \neq u_h$. A similar situation occurs in Example 7.3. Notice also the "built-in localization" of $\|(\chi - u_h)^+\|_{0,\infty;\Omega}$.

Remark 5.10 (Logarithmic factor)**.** The presence of a logarithmic factor in $\mathcal{E}_h$ is unavoidable in the a priori error analysis in 2d and 3d [10], [14]. Its power may be improved from 2 to 1, as in the case of smooth or convex domains.

Remark 5.11 (1d)**.** The pointwise error estimate (5.7) can be simplified in 1d. First, we can remove the jumps in the residual R_∞ of (3.7), and also take $\Pi_h = I_h$ in the definition (3.1) of $\tilde{\sigma}_h$ because I_h is stable in $H_0^1(\Omega)$. Secondly, we can remove the log factor in $\mathcal{E}_h$ because the regularized Green's function is uniformly in $W_1^2(\Omega)$.

6. Lower bounds

Once an a posteriori error estimator is obtained, the question arises whether or not this estimator may overestimate the error. The purpose of this section is to investigate this issue for the estimator $\mathcal{E}_h$ of the Theorem 5.4.

We call an estimator (or some part of it) *globally efficient*, if it is dominated by the global error and the global data approximation. Similarly, we call an estimator (or some part of it) *locally efficient*, if the corresponding local indicator is dominated by the local error and the local data approximation. Global efficiency is a desirable property for stopping an adaptive procedure, while local efficiency protects against over-refinement.

The following notions of data approximation will appear later:

- The oscillation $\|h^2(f - \bar{f})\|_{0,\infty;\Omega}$ of the load function f, where $\bar{f}$ is the piecewise constant function defined by $\bar{f}_{|T} = |T|^{-1} \int_T f$ for all $T \in \mathcal{T}_h$;

- The discrete obstacle oscillation $\|h\,[\![\partial_\nu \chi_h]\!]\|_{0,\infty;\Omega}$; hereafter, we set

$$\|h\,[\![\partial_\nu \chi_h]\!]\|_{0,\infty;\omega} := \max\{h_S\,[\![\partial_\nu \chi_h]\!]_S \mid S \in \mathcal{S}_h \text{ with } S \cap \operatorname{int}(\omega) \neq \emptyset\}$$

  for any subset ω of Ω.
- The obstacle approximation $\|(\chi_h - \chi)^+\|_{0,\infty;\Omega}$.

For an open subset $\omega \subset \Omega$ and $\rho \in W^*$, we define the local seminorm

$$\|\rho\|_{-2,\infty;\omega} := \sup\big\{\langle \rho,\, \varphi\rangle \mid \varphi \in W \text{ with } |D^2\varphi|_{\mathrm{var}}(\omega) \leq 1 \text{ and } \operatorname{supp}\varphi \subset \bar{\omega}\big\}.$$

6.1. **Efficiency of Localized Residual.** We intend to show a lower bound for the localized residual $\|h^2 R_\infty\|_{0,\infty;\Omega}$ and a few other terms in (5.7). To combine definitions (2.6) and (3.1), we will rely on a variant of Verfürth's argument (see Verfürth [19] and also Nochetto [11]). In fact, we construct suitable bubble functions which, for simplicity, belong to $W_1^2(\Omega) \cap \mathring{H}^1(\Omega) \subset W$ instead of W.

We first consider (2.6) and investigate (as promised) a suitable choice of radius for the ball $B(z)$. Such radius is $\rho_z := \max\{r > 0 \mid B(z;r) \subset \mathcal{U}_h(z)\}$ in [3], but it can be reduced at the expense of a larger stability constant. In order to obtain additional properties of Π_h, and thus of $\tilde{\sigma}_h$, we redefine the radius of $B(z)$ as follows.

Lemma 6.1 (Retracted bubble functions). *Set $B(z) := B(z;\delta\rho_z)$ in (2.6). Then there exists $\delta \in (0,1)$ depending only on the shape-regularity $\gamma(\mathcal{T}_h)$ and, for all $T \in \mathcal{T}_h$ and $S \in \mathcal{S}_h$, there exist bubble functions b_T and b_S in $W_1^2(\Omega) \cap \mathring{H}^1(\Omega)$ such that the following properties are valid for all $\varphi \in L_1(\Omega)$, $\varphi_T \in \mathbb{P}^1(T)$:*

$$\Pi_h(\varphi b_T) = 0, \tag{6.1a}$$

$$\|\varphi_T\|_{0,\infty;T} \preccurlyeq \sup\left\{\int_T \varphi_T \zeta_T b_T \mid \zeta_T \in \mathbb{P}^1(T),\, \|\zeta_T\|_{0,1;T} \leq 1\right\}, \tag{6.1b}$$

$$\|\varphi_T b_T\|_{2,1;T} \preccurlyeq h_T^{-2}\|\varphi_T b_T\|_{0,1;T} \preccurlyeq h_T^{-2}\|\varphi_T\|_{0,1;T}, \tag{6.1c}$$

$$\Pi_h(\varphi b_S) = 0, \tag{6.2a}$$

$$1 \preccurlyeq |S|^{-1}\int_S b_S, \tag{6.2b}$$

$$\|b_S\|_{2,1;T} \preccurlyeq h_S^{-2}\|b_S\|_{0,1;T} \preccurlyeq h_S^{-1}|S|, \qquad \text{if } S \subset \partial T. \tag{6.2c}$$

Proof. **1.** We first explain the idea informally. In order to obtain (6.1a) and (6.2a), we ensure that the balls $B(z)$ in (2.6) and the supports of the bubble functions b_T and b_S do not overlap. To this end, the support of a bubble function will be contained in a sufficiently small ball centered at the barycenter x_T or x_S of the corresponding simplex T or side S.

2. Given $z \in \mathring{\mathcal{N}}_h$, we define

$$r_z := \min\big\{|z - x_T|, |z - x_S| \mid T \subset \mathcal{U}_h(z),\, S \cap \operatorname{int}\big(\mathcal{U}_h(z)\big) \neq \emptyset\big\}. \tag{6.3}$$

Note that the barycenters of simplices and sides not appearing in (6.3) have at least distance ρ_z from z. Elementary geometry yields $r_z \succcurlyeq \rho_z$ and thus allows the following definition: let $\delta \in (0,1)$ be the largest constant, depending on the shape-regularity $\gamma(\mathcal{T}_h)$, such that $\frac{1}{2} r_z \geq \delta\rho_z$ for all $z \in \mathring{\mathcal{N}}_h$. This definition implies that the balls $B(z, \delta\rho_z)$ stay away from the barycenters of simplices and sides.

3. To be more specific, let $0 < \mu < 1$ be a constant solely depending on shape-regularity such that

$$\mu h_T \leq \min\{\tfrac{1}{2} r_z \mid z \in \mathring{\mathcal{N}}_h \cap T\} \qquad \text{for all } T \in \mathcal{T}_h.$$

The same holds for all $S \in \mathcal{S}_h$. We thus infer that the balls $B(z, \delta\rho_z)$ and $B(x_T, \mu h_T)$ do not overlap irrespective of the location of z and x_T. Moreover, this remains true, if we replace $B(x_T, \mu h_T)$ by $B(x_S, \mu h_T) \cap T$, where S is a side of a simplex T.

4. We now construct the bubble function b_T for any simplex $T \in \mathcal{T}_h$. Let $\tilde{T}$ be the retraction of T by factor μ with respect to its barycenter x_T. We then define

$$b_T(x) = \begin{cases} \prod_{k=1}^{d+1} \lambda_k^2(x), & \text{if } x \in \tilde{T}, \\ 0, & \text{if } x \in \Omega \setminus \tilde{T}, \end{cases}$$

where $\lambda_1, \dots, \lambda_{d+1}$ are the barycentric coordinates of $\tilde{T}$. Squaring the barycentric coordinates ensures that b_T is continuously differentiable and so $b_T \in W_1^2(\Omega)$; compare with [19, Remark 3.6]. In view of step 3, we have $\operatorname{supp} b_T \cap B(z; \delta\rho_z) = \emptyset$ for all interior nodes $z \in \mathring{\mathcal{N}}_h$, whence (6.1a) is valid. To establish (6.1b) and (6.1c) we proceed as in [19, Lemma 3.3] upon noticing that the quotient $h_{\tilde{T}}/h_T = \mu$ depends only on the shape-regularity $\gamma(\mathcal{T}_h)$.

5. We now construct the bubble function b_S for any inter-element side $S \in \mathcal{S}_h$. Let T_1 and T_2 be the two adjacent simplices whose intersection is S. Let $\tilde{S}$ be the retraction of S by factor μ with respect to its barycenter x_S. Let $\tilde{T}_1$ and $\tilde{T}_2$ be the tetrahedrals similar to T_1 and T_2 whose intersection is $\tilde{S}$. We define

$$b_S(x) = \begin{cases} \prod_{k=1}^{d} \lambda_{1,k}^2(x) \lambda_{2,k}^2(x), & \text{if } x \in \tilde{T}_1 \cup \tilde{T}_2, \\ 0, & \text{if } x \in \Omega \setminus (\tilde{T}_1 \cup \tilde{T}_2), \end{cases}$$

where $\lambda_{i,1}, \dots, \lambda_{i,d+1}$ are the (extended) barycentric coordinates of $\tilde{T}_i$, with a numbering such that $\lambda_{i,d+1}$ corresponds to the node not contained in $\tilde{S}$, $i = 1, 2$. Again, multiplying and squaring the barycentric coordinates ensures $b_S \in W_1^2(\Omega)$. In view of step 3, $\operatorname{supp} b_S \cap B(z; \delta\rho_z) = \emptyset$ for every interior $z \in \mathring{\mathcal{N}}_h$ and thus (6.2a) is valid. Since $h_{\tilde{S}}/h_S = \mu$, (6.2b) and (6.2c) can be proved similarly to (6.1b) and (6.1c). □

We choose δ as in the preceding lemma and let Π_h be the interpolation operator of (2.6) with $B(z) = B(z; \delta\rho_z)$. Using (6.1a) and (6.2a) in definition (3.1) yields

$$\langle \tilde{\sigma}_h, \varphi b_T \rangle = \int_{\Lambda_h} \sigma_h \varphi b_T, \quad \langle \tilde{\sigma}_h, \varphi b_S \rangle = \int_{\Lambda_h} \sigma_h \varphi b_S \qquad \text{for all } \varphi \in L_2(\Omega); \tag{6.4}$$

that is there is no contribution from the discrete non-contact set $\Omega \setminus \Lambda_h$. After these preliminaries, we are ready to prove our main assertion.

Proposition 6.2 (Efficiency I). *The localized residual $\|h^2 R_\infty\|_{0,\infty;\Omega}$, the boundary value approximation $\|I_h g - g\|_{0,\infty;\partial\Omega}$, and $\|(\chi - u_h)^+\|_{0,\infty;\Omega}$ are globally and locally efficient. In particular, for any $T \in \mathcal{T}_h$, there holds*

$$\begin{aligned} h_T^2 \|R_\infty\|_{0,\infty;T} + \|I_h g - g\|_{0,\infty;\partial\Omega\cap T} + \|(\chi - u_h)^+\|_{0,\infty;T} \\ \preccurlyeq \|u - u_h\|_{0,\infty;T^*} + \|\sigma - \tilde{\sigma}_h\|_{-2,\infty;T^*} + \|h^2(f - \bar{f})\|_{0,\infty;T^*}, \end{aligned} \tag{6.5}$$

where T^* is the union of all simplices that share at least one side with T.

Proof. **1.** Since $g - I_h g = u - u_h$ on $\partial\Omega$, the bound for the middle term in (6.5) is trivial. Since $(\chi - u_h)^+ \le (u - u_h)^+$, the bound for the rightmost term in (6.5) follows immediately. It remains to deal with the localized residual term R_∞.

2. We next estimate the interior residual. Given $T \in \mathcal{T}_h^0$, and noticing that $f_T - \sigma_h|_T \in \mathbb{P}^1(T)$, we choose a function $\zeta_T \in \mathbb{P}^1(T)$ by means of (6.1b) such that

$$\|f_T - \sigma_h\|_{0,\infty;T} \eqsim \int_T (f_T - \sigma_h)\zeta_T b_T \quad \text{and} \quad \|\zeta_T\|_{0,1;T} \leq 1.$$

In view of (6.4) with $\varphi = \zeta_T$, we can write

$$\int_T (f_T - \sigma_h)\zeta_T b_T = \int_T (f - \tilde{\sigma}_h)\zeta_T b_T + \int_T (f_T - f)\zeta_T b_T,$$

whence, making use of (3.3) and $\langle \nabla u_h, \nabla(\zeta_T b_T)\rangle = 0$, we arrive at

$$\int_T (f_T - \sigma_h)\zeta_T b_T = \langle \mathcal{G}_h,\, \zeta_T b_T\rangle + \int_T (f_T - f)\zeta_T b_T.$$

Invoking (3.11) and (6.1c), adding and substracting f on the left-hand side and using the triangle inequality, we infer that

$$h_T^2 \|f - \sigma_h\|_{0,\infty;T} \eqsim \|u_h - u\|_{0,\infty;T} + \|\tilde{\sigma}_h - \sigma\|_{-2,\infty;T} + h_T^2 \|f_T - f\|_{0,\infty;T}.$$

If instead $T \in \mathcal{T}_h^+$, the above argument also applies upon realizing from (6.4) that

$$\int_T f_T \zeta_T b_T = \int_T (f - \tilde{\sigma}_h)\zeta_T b_T + \int_T (f_T - f)\zeta_T b_T.$$

In this case, we deduce that

$$h_T^2 \|f\|_{0,\infty;T} \eqsim \|u_h - u\|_{0,\infty;T} + \|\tilde{\sigma}_h - \sigma\|_{-2,\infty;T} + h_T^2 \|f_T - f\|_{0,\infty;T}.$$

3. We now estimate the jump residual $h_S J_S$ for any inter-element side S, where $J_S := [\![\partial_\nu u_h]\!]_S$ is constant. According to (6.2b), there exists $\alpha_S \in \mathbb{R}$ such that

$$\|J_S\|_{0,\infty;S} \eqsim \int_S J_S \alpha_S b_S, \qquad \|\alpha_S\|_{0,1;S} \leq 1.$$

Therefore, integrating by parts and making use of (3.3) as well as (6.4), we deduce

$$\|J_S\|_{0,\infty;S} \eqsim -\int_{\omega_S} \nabla u_h \nabla(\alpha_S b_S) = \langle \mathcal{G}_h,\, \alpha_S b_S\rangle - \int_{\omega_S} (f - \sigma_h \mathbf{1}_{\Lambda_h})(\alpha_S b_S),$$

where ω_S denotes the union of the two simplices that contain S and $\mathbf{1}_{\Lambda_h}$ is the characteristic function of Λ_h. In light of (6.2c), we conclude the desired estimate

$$h_S \|J_S\|_{0,\infty;S} \eqsim \|u - u_h\|_{0,\infty;\omega_S} + \|\sigma - \tilde{\sigma}_h\|_{-2,\infty;\omega_S} + h_S^2 \|f - \sigma_h \mathbf{1}_{\Lambda_h}\|_{0,\infty;\omega_S}.$$

4. Finally, combining the preceding steps and noticing $h_S \leq h_T$ for $S \subset \partial T$ completes the proof. □

6.2. **Efficiency of $\|(u_h - \chi)^+\|_{0,\infty;\{\sigma_h<0\}}$.** Before discussing the efficiency properties of $\|(u_h - \chi)^+\|_{0,\infty;\{\sigma_h<0\}}$, we recall Remark 4.3: to obtain computable error indicators we are forced to substitute the term $\|(u_h - u)^+\|_{0,\infty;\{\sigma_h<0\}}$ with $\|(u_h - \chi)^+\|_{0,\infty;\{\sigma_h<0\}}$. The first term $\|(u_h - u)^+\|_{0,\infty;\{\sigma_h<0\}}$ is clearly locally and globally efficient, while the computable term $\|(u_h - \chi)^+\|_{0,\infty;\{\sigma_h<0\}}$ has the following efficiency properties.

Proposition 6.3 (Efficiency II). *Let $T \in \mathcal{T}_h$ with $T \cap \{\sigma_h < 0\} \neq \emptyset$. Then the following local lower bounds hold for $\|(u_h - \chi)^+\|_{0,\infty;T}$:*

(i) *If $T \subset \{u_h = \chi_h\}$, then $\|(u_h - \chi)^+\|_{0,\infty;T} \leq \|(\chi_h - \chi)^+\|_{0,\infty;T}$.*

(ii) *Otherwise, if $T \cap \{u_h > \chi_h\} \neq \emptyset$, then*

$$\begin{aligned} \|(u_h - \chi)^+\|_{0,\infty;T} \eqsim\ & \|u - u_h\|_{0,\infty;\mathcal{U}_h(T)} + \|\sigma - \tilde{\sigma}_h\|_{-2,\infty;\mathcal{U}_h(T)} \\ & + \|h(f - \bar{f})\|_{0,\infty;\mathcal{U}_h(T)} + \|(\chi_h - \chi)^+\|_{0,\infty;T} + \|h\,[\![\partial_\nu \chi_h]\!]\,\|_{0,\infty;\mathcal{U}_h(T)}. \end{aligned} \tag{6.6}$$

The non-trivial lower bound (ii) of Proposition 6.3 relies on the following discrete counterpart of (2.9) in Baiocchi [2], which is a statement about quadratic growth of any non-negative function with bounded second derivatives.

Lemma 6.4 (Discrete quadratic growth). *Let $v_h \in \mathbb{V}_h$ with $v_h \geq 0$ and $v_h(z) = 0$ for some interior node $z \in \mathring{\mathcal{N}}_h$. Then*

$$\|v_h\|_{0,\infty;\mathcal{U}_h(z)} \preccurlyeq h_z \| \, [\![\partial_\nu v_h]\!] \, \|_{0,\infty;\mathcal{U}_h(z)} \tag{6.7}$$

holds, where $h_z := \max\{h_T;\ T \in \mathcal{T}_h$ with $T \ni z\}$ and the constant hidden in $\preccurlyeq$ can be bounded by the number of simplices in $\mathcal{U}_h(z)$.

Proof. **1.** Combining $v_h \geq 0$, $v_h(z) = 0$, and the piecewise linear character of v_h, we conclude that there is an $x \in \mathcal{N}_h \cap \partial\mathcal{U}_h(z)$ such that

$$\|v_h\|_{0,\infty;\mathcal{U}_h(z)} = v_h(x). \tag{6.8}$$

2. Define

$$\tau := \frac{x - z}{|x - z|}$$

and choose one $T \in \mathcal{T}_h$ with $x, z \in T$. Since z is an interior node, there exist a simplex $\tilde{T} \subset \mathcal{U}_h(z)$ and an $\varepsilon > 0$ such that $\tilde{x}, z \in \tilde{T}$ holds with $\tilde{x} := z - \varepsilon\tau$ (compare Figure 6.1). Observing that

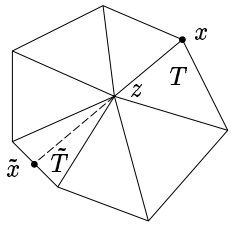

FIGURE 6.1. Neighbourhood $\mathcal{U}_h(z)$ with points x, $\tilde{x}$ and simplices T, $\tilde{T}$ in the case $d = 2$.

$$0 \leq v_h(x) = v_h(x) - v_h(z) = |x - z| \, \nabla v_{h|T} \cdot \tau$$

and

$$0 \leq v_h(\tilde{x}) - v_h(z) = -\varepsilon \, \nabla v_{h|\tilde{T}} \cdot \tau$$

holds, we conclude

$$\nabla v_{h|T} \cdot \tau \geq 0 \qquad \text{and} \qquad -\nabla v_{h|\tilde{T}} \cdot \tau \geq 0. \tag{6.9}$$

This implies

$$\begin{aligned} v_h(x) &\leq |x - z| \left(\nabla v_{h|T} \cdot \tau - \nabla v_{h|\tilde{T}} \cdot \tau \right) \\ &= |x - z| \left| (\nabla v_{h|T} - \nabla v_{h|\tilde{T}}) \cdot \tau \right| \leq |x - z| \left| \nabla v_{h|T} - \nabla v_{h|\tilde{T}} \right|. \end{aligned} \tag{6.10}$$

3. Let $(T_i)_{i=0}^n \subset \mathcal{U}_h(z)$ be a sequence of simplices, connecting T and $\tilde{T}$, i.e. $T_0 = T$, $T_n = \tilde{T}$, and $T_{i-1} \cap T_i = S_i \in \mathcal{S}_h$ is a common side of T_{i-1} and T_i for $i = 1, \ldots, n$. Denote by ν_i the unit normal of S_i in the direction from T_{i-1}

to T_i. Since v_h is globally continuous, the jump of tangential derivatives across inter-element sides is 0 and thus

$$\nabla v_{h|T} - \nabla v_{h|\tilde{T}} = \sum_{i=1}^{n} \left(\nabla v_{h|T_{i-1}} - \nabla v_{h|T_i} \right) = \sum_{i=1}^{n} \left(\nabla v_{h|T_{i-1}} - \nabla v_{h|T_i} \right) \cdot \nu_i \, \nu_i.$$

Using (6.10) we further see that

$$v_h(x) \leq |x - z| \left| \nabla v_{h|T} - \nabla v_{h|\tilde{T}} \right| \leq n \, h_z \, \| \, [\![\partial_\nu v_h]\!] \, \|_{0,\infty;U_h(z)}.$$

Since the number of elements n in $\mathcal{U}_h(z)$ is uniformly bounded for shape-regular partitions $\mathcal{T}_h$, the proof is thus finished. □

Proof of Proposition 6.3. The statement (i) is trivial. In order to prove statement (ii), let $T \in \mathcal{T}_h$ satisfy $T \cap \{\sigma_h < 0\}$, $T \cap \{u_h > \chi_h\} \neq \emptyset$. We first observe that

$$\|(u_h - \chi)^+\|_{0,\infty;T} \leq \|u_h - \chi_h\|_{0,\infty;T} + \|(\chi_h - \chi)^+\|_{0,\infty;T}$$

and, therefore, it remains to estimate $\|u_h - \chi_h\|_{0,\infty;T}$. Since $T \cap \{\sigma_h < 0\} \neq \emptyset$, there exists a node $z \in \mathcal{N}_h \cap T$ with $\sigma_h(z) < 0$ and so $u_h(z) = \chi_h(z)$. Moreover, due to $T \cap \{u_h > \chi_h\} \neq \emptyset$ and the definition of σ_h, the node z has to be an interior node: $z \in \mathring{\mathcal{N}}_h$. Consequently, we can apply Lemma 6.4 to obtain

$$\|u_h - \chi_h\|_{0,\infty;T} \preccurlyeq \|h \, [\![\partial_\nu u_h]\!] \, \|_{0,\infty;\mathcal{U}_h(T)} + \|h \, [\![\partial_\nu \chi_h]\!] \, \|_{0,\infty;\mathcal{U}_h(T)}.$$

Finally, we conclude by estimating $\|h \, [\![\partial_\nu u_h]\!] \, \|_{0,\infty;\mathcal{U}_h(T)}$ with the help of (6.5). □

The significance of the lower bound (6.6) hinges on the behavior of the terms $\|(\chi_h - \chi)^+\|_{0,\infty;T}$ and $\|h \, [\![\partial_\nu \chi_h]\!] \, \|_{0,\infty;\mathcal{U}_h(T)}$. In the next remark, we show that these terms are of second order, if the obstacle χ is smooth.

Remark 6.5 (Smooth obstacles)**.** If $\chi \in W^2_\infty(\mathcal{U}_h(T))$ for $T \in \mathcal{T}_h$, then we claim

$$\|(\chi_h - \chi)^+\|_{0,\infty;T} + \|h \, [\![\partial_\nu \chi_h]\!] \, \|_{0,\infty;\mathcal{U}_h(T)} \preccurlyeq h_T^2 \, \|D^2 \chi\|_{0,\infty;\mathcal{U}_h(T)}.$$

By standard estimates for the Lagrange interpolation operator, we obtain

$$\|(\chi_h - \chi)^+\|_{0,\infty;T} \leq \|\chi_h - \chi\|_{0,\infty;T} \preccurlyeq h_T^2 \, \|D^2 \chi\|_{0,\infty;T}$$

as well as (use that $[\![\partial_\nu \chi_h]\!] = [\![\partial_\nu (\chi_h - \chi)]\!]$)

$$\|h \, [\![\partial_\nu \chi_h]\!] \, \|_{0,\infty;\mathcal{U}_h(T)} \preccurlyeq \|h \nabla (\chi_h - \chi)\|_{0,\infty;\mathcal{U}_h(T)} \preccurlyeq h_T^2 \, \|D^2 \chi\|_{0,\infty;\mathcal{U}_h(T)}.$$

We summarize the above statements of this subsection as follows: *the term* $\|(u_h - \chi)^+\|_{0,\infty;\{\sigma_h < 0\}}$ *is locally and globally efficient for smooth obstacles.*

6.3. **Efficiency of Quadrature Estimator.** We finally investigate the estimator $\|h^2 \nabla \sigma_h\|_{0,d;\Lambda_h}$ caused by mass lumping $\langle \cdot, \cdot \rangle_h$ in the definition of σ_h. This in turn guarantees the crucial non-positivity and complementarity nodal properties of σ_h.

Proposition 6.6 (Efficiency III)**.** *The quadrature estimator* $\|h^2 \nabla \sigma_h\|_{0,d;\Lambda_h}$ *is locally efficient. In particular, for any* $T \in \mathcal{T}_h^0$*, there holds*

$$\|h^2 \nabla \sigma_h\|_{0,d;T} \preccurlyeq \|u - u_h\|_{0,\infty;T} + \|\sigma - \tilde{\sigma}_h\|_{-2,\infty;T} + \|h^2 (f - f_T)\|_{0,\infty;T}. \tag{6.11}$$

Proof. Let $T \in \mathcal{T}_h^0$. We first observe that an inverse estimate yields

$$h_T^2 \|\nabla \sigma_h\|_{0,d;T} = h_T^2 \|\nabla (\sigma_h - f_T)\|_{0,d;T} \preccurlyeq h_T^2 \|f - \sigma_h\|_{0,\infty;T} + h_T^2 \|f - f_T\|_{0,\infty;T}.$$

We finally deduce (6.11) with the help of step 2 in the proof of Proposition 6.2. □

Note that, in contrast to the other local estimates in Propositions 6.2 and 6.3, the local estimate (6.11) does *not* obviously imply global efficiency. This is due to the fact that switching to the corresponding global quantities requires summing on the left-hand side of (6.11) but maximizing on its right-hand side. Nevertheless our numerical results of §7.2 display global efficiency for the quadrature estimator, if the marking strategy takes into account the "different accumulation" (see §7.1).

We conclude this section by clarifying the reason for the different integrabilities arising in (6.11). Let Π_h^* be the adjoint operator of Π_h and consider $\|\Pi_h^* \mathcal{Q}_h\|_{-2,\infty;\Omega}$. This quantity could be used to bound the term $\langle \mathcal{Q}_h, \Pi_h \varphi \rangle$ in the representation formula (3.5) and is *globally* efficient. To prove this claim, let $\varphi \in W$ and compute

$$\begin{aligned} |\langle \mathcal{Q}_h, \Pi_h \varphi \rangle| &= |\langle \mathcal{G}_h, \varphi \rangle - \langle \mathcal{R}_h, \varphi - \Pi_h \varphi \rangle| \\ &\le \big(\|\mathcal{G}_h\|_{-2,\infty;\Omega} + \|h^2 R_\infty\|_{0,\infty;\Omega} \big) \, |D^2 \varphi|_{\mathrm{var}}(\Omega) \\ &\preccurlyeq \big(\|u - u_h\|_{0,\infty;\Omega} + \|\sigma - \tilde{\sigma}_h\|_{-2,\infty;\Omega} + \|h^2 (f - \bar{f})\|_{0,\infty;\Omega} \big) \, |D^2 \varphi|_{\mathrm{var}}(\Omega) \end{aligned}$$

by using (3.5), (3.8), (3.11), and (6.5). However, $\|\Pi_h^* \mathcal{Q}_h\|_{-2,\infty;\Omega}$ is global and non-computable. Unfortunately, the functional $\mathcal{Q}_h \in \mathring{\mathbb{V}}_h^*$ does not exhibit enough cancellation to switch to $|D^2 \Pi_h \varphi|_{\mathrm{var}}$ *directly* in (3.9), and so to $|D^2 \varphi|_{\mathrm{var}}$. We are thus forced to use a Sobolev-type inequality in (3.9) which bounds $\|\Pi_h^* \mathcal{Q}_h\|_{-2,\infty;\Omega}$ in terms of local computable quantities. A similar situation occurs for unconstrained linear problems with quadrature, which does not seem to be investigated.

7. Numerical Experiments

In this section we present several simulations with smooth and rough obstacles and illustrate the role of the various terms of $\mathcal{E}_h$ in (5.7). We first compare $\mathcal{E}_h$ with the computable part $\|u - u_h\|_{0,\infty;\Omega}$ of the error (see Example 7.2), and later discuss the impact of the non-computable error $\|\sigma - \tilde{\sigma}_h\|_{-2,\infty;\Omega}$ (see Example 7.4).

7.1. **Implementation.** The solver for the obstacle problem (1.1) is implemented within the finite element toolbox ALBERT [15, 16], which resorts to bisection and thus guarantees (2.1). We solve the resulting *nonlinear* discrete system with the projective SOR method analyzed in [5]. To implement the estimator, we first compute σ_h which involves assembling and solving one additional *linear system* with diagonal system matrix.

In our simulations we have replaced the factors $C_i |\log h_{\min}|^2$ $(i = 1, 2)$ of $\mathcal{E}_h$ by constants $\tilde{C}_0 = 0.1$ and $\tilde{C}_1 = 0.01$, namely we have used the more practical estimator

$$\begin{aligned} \tilde{\mathcal{E}}_h = \tilde{C}_0 \|h^2 R_\infty\|_{0,\infty;\Omega} + \tilde{C}_1 \|h^2 \nabla \sigma_h\|_{0,d;\Lambda_h} \\ + \|(\chi - u_h)^+\|_{0,\infty;\Omega} + \|(u_h - \chi)^+\|_{0,\infty;\{\sigma_h < 0\}} + \|g - I_h g\|_{0,\infty;\partial\Omega}. \end{aligned} \tag{7.1}$$

Note, that the last three terms actually enter $\mathcal{E}_h$, and so $\tilde{\mathcal{E}}_h$, without any constant. For terms involving non-polynomial data, the maximum norm is approximated by evaluating element point-values at the Lagrange nodes for 7th order polynomials.

We employ the maximum strategy to mark elements for refinement, which seems adequate for error control in the maximum norm. Since the L_d quadrature indicator $\eta_{d;T} := \tilde{C}_1 \|h^2 \nabla \sigma_h\|_{0,d;\Lambda_h \cap T}$ exhibits *different accumulation* in Ω than the other L_∞

indicators of $\tilde{\mathcal{E}}_h$, namely,

$$\eta_{\infty;T} := \tilde{C}_0 \|h^2 R_\infty\|_{0,\infty;T} + \|(\chi - u_h)^+\|_{0,\infty;T} + \|(u_h - \chi)^+\|_{0,\infty;\{\sigma_h<0\}\cap T} + \|g - I_h g\|_{0,\infty;\partial\Omega\cap T},$$

we resort to two marking loops. We *first* mark solely according to $\{\eta_{\infty;T}\}_{T\in\mathcal{T}_h}$, and *next* according to $\{\eta_{d;T}\}_{T\in\mathcal{T}_h^0}$ provided quadrature dominates the estimator. This 2-step strategy displays an optimal reduction rate of error and estimator in our experiments of §7.2.

7.2. **Example: Constant Obstacle.** We consider a constant obstacle $\chi \equiv 0$ on the domain $\Omega = (-1,1)^d$ and, for $r < 1$, the forcing term

$$f(x) = \begin{cases} -4\left(2\,|x|^2 + d\,(|x|^2 - r^2)\right), & |x| > r \\ -8\,r^2\left(1 - (|x|^2 - r^2)\right), & |x| \le r \end{cases}$$

and Dirichlet value $g(x) = (|x|^2 - r^2)^2$. Hence, the exact solution of (1.1) reads

$$u(x) = \left(\max\{|x|^2 - r^2, 0\}\right)^2.$$

The corresponding measure σ is absolutely continuous with respect to the Lebesgue measure and has a bounded Radom-Nikodym derivative with a discontinuity across the free boundary.

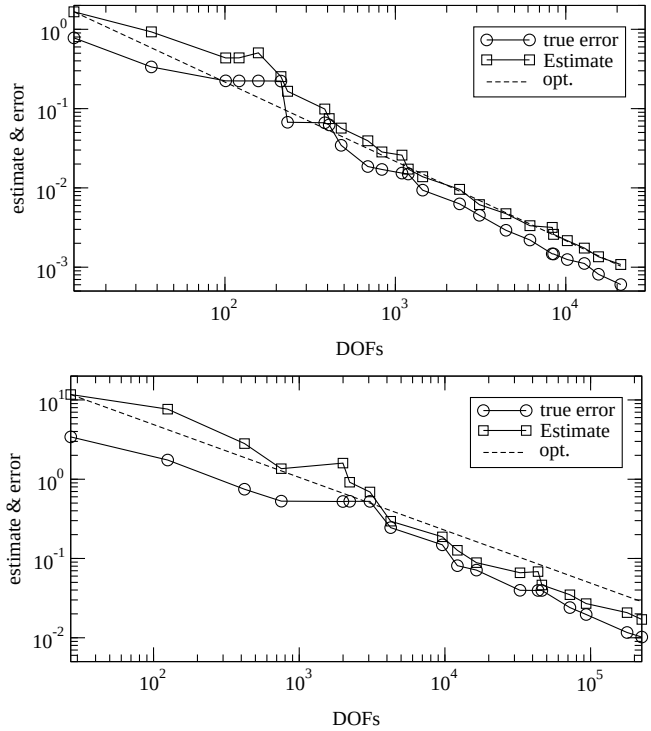

FIGURE 7.1. Example 7.2: Estimator and true error $\|u-u_h\|_{0,\infty;\Omega}$ for $d = 2$ (top) and $d = 3$ (bottom) for $\chi = 0$ vs. DOFs (Degrees Of Freedom). The optimal decay is indicated by the dotted line with slope $-2/d$.

Figure 7.1 shows a comparison of the error and the estimator for the 2d and 3d simulations with $r = 0.7$. This picture corroborates that the estimator always provides an upper bound for the error (reliability) and the average decay of both error and estimator is the same (efficiency). It also shows the asymptotic relation $\|u - u_h\|_{0,\infty;\Omega} = C\ \mathrm{DOFs}^{-2/d}$ typical of quasi-optimal meshes and thus of quasi-optimal numerical complexity. In the log-log plot the optimal decay of $\|u-u_h\|_{0,\infty;\Omega}$ is a straight line with slope $-2/d$. This (dashed) line is also plotted in Figure 7.1.

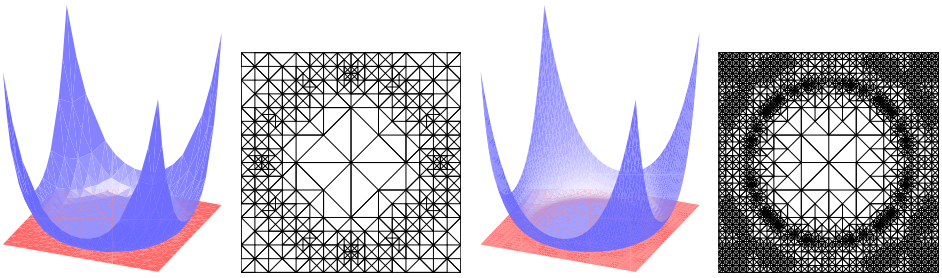

FIGURE 7.2. Example 7.2: Discrete solutions, constant obstacle, and corresponding grids for $d = 2$ for adaptive iterations $j = 7, 15$.

Figure 7.2 depicts the discrete solution and the corresponding adaptive grid for two adaptive iterations in 2d. For the 3d simulation of Figure 7.3, the cuboid $(0,1)^2 \times (-1,1)$ has been cut out of the domain Ω and the grid has been plotted on the boundary on the resulting domain. Note that there is nearly no refinement inside the coincidence set although f does not vanish there (localization). The discontinuity of σ across the free boundary and the presence of $\|\sigma - \tilde{\sigma}_h\|_{-2,\infty;\Omega}$ in the error are responsible for the additional refinement nearby.

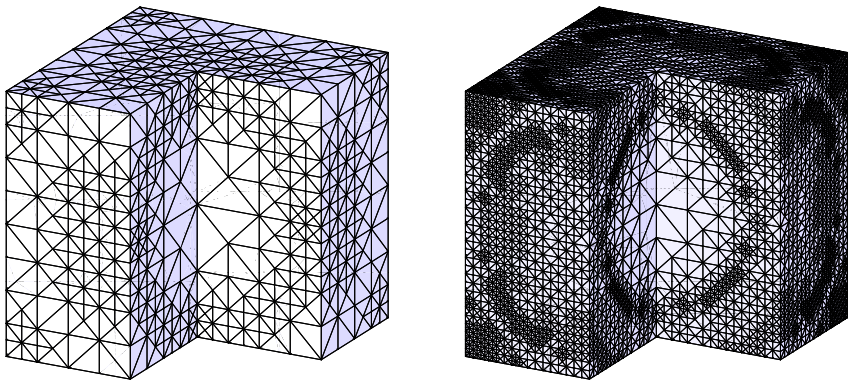

FIGURE 7.3. Example 7.2: Grids for $d = 3$ of the adaptive iterations $j = 7, 15$ on $\partial\big(\Omega\backslash\big((0,1)^2 \times (-1,1)\big)\big)$.

7.3. **Example: Obstacle with a Cusp.** We consider data Ω, f, and g of Example 7.2, but with an obstacle χ with an upward cusp at the origin, which happens to be a node (see Figure 7.4). The corresponding measure σ is singular with respect to the Lebesgue measure with a mass supported at the origin — the contact set.

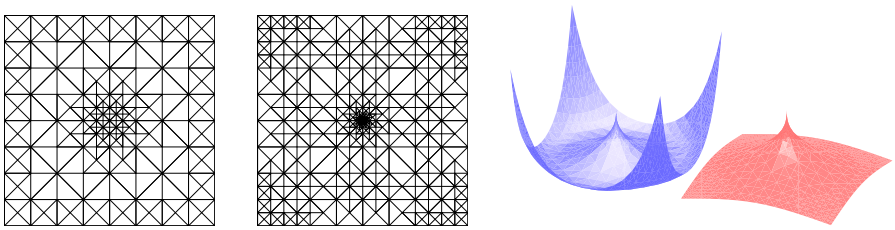

FIGURE 7.4. Example 7.3: Grids for adaptive iterations $j = 5, 8$, and discrete solution and obstacle for $j = 8$.

We observe that the refinement is driven by the first two terms in (7.1) as well as the forth. The latter is indeed essential to detect the strong discrepancy between u_h and χ near the tip, and thus refine accordingly. The third term in (7.1) is zero because the obstacle χ is concave and the tip is located at a node of the grid. We stress that the localization built into the forth term is clearly reflected in a localized refinement.

7.4. **Example: Lipschitz Obstacles.** We consider $f = -5$ and $g = 0$ on the domain $\Omega = \{(x_1, \dots, x_d) \mid \sum_{i=1}^{d} |x_i| < 1\}$, $d = 2$ or 3, together with two Lipschitz obstacles χ. The first one is

$$\chi(x) := \operatorname{dist}(x, \partial\Omega) - \tfrac{1}{5}.$$

The function χ is piecewise linear and the graph is a pyramid in 2d. The corresponding measure σ is singular with respect to the Lebesgue measure since it has mass supported along the edges of the obstacle within the contact set.

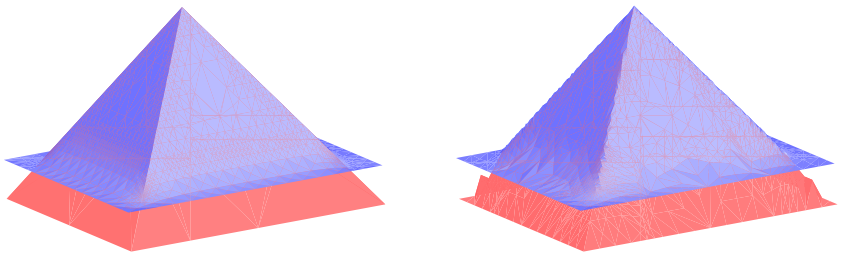

FIGURE 7.5. Example 7.4: Discrete solution and obstacle for $d = 2$ on grids aligned with the edges of the obstacle (left) and non-aligned (right).

Figure 7.5 displays u_h and χ_h for $d = 2$ over two meshes, one aligned and the other non-aligned with the edges of χ: in the latter the representation χ_h of χ is rather crude. Even though the aligned meshes provide excellent approximability of χ and u, there is still a strong refinement along the edges within the contact set due to poor approximation of σ in the non-computable part of the error (see left of Figure 7.6). In contrast, the refinement for the non-aligned meshes is instead due to lack of resolution of χ and thus of u (see right of Figure 7.6). Note that the non-aligned grids do not satisfy the discrete maximum principle.

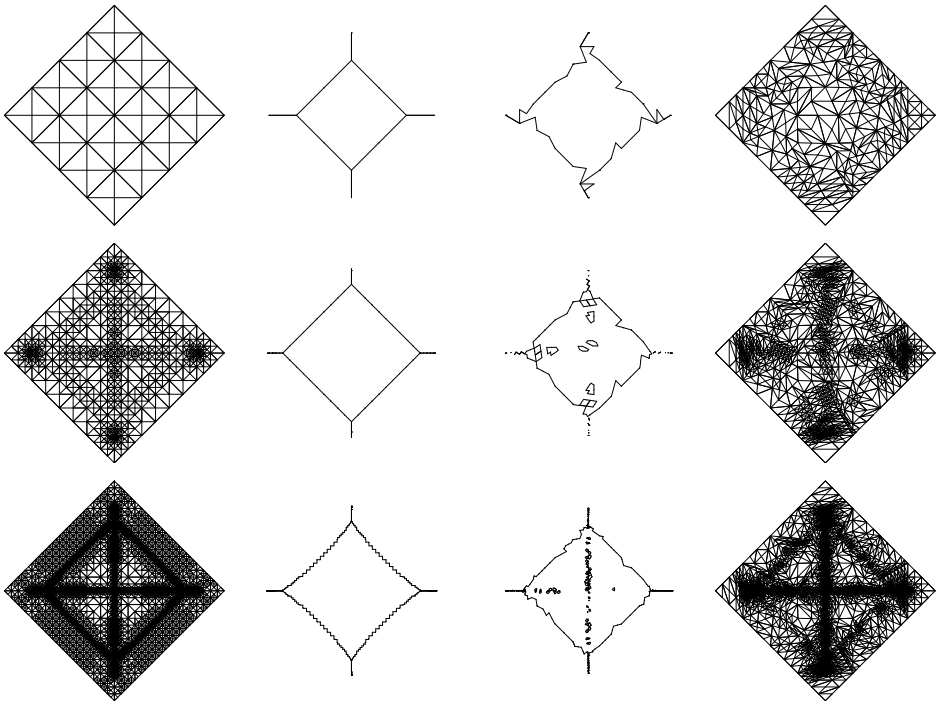

FIGURE 7.6. Example 7.4: Grids and $\partial\{u_h = \chi_h\}$ for $d = 2$ on grids aligned to the edges of the obstacle (left) and non-aligned (right) for adaptive iterations $j = 1, 7, 15$.

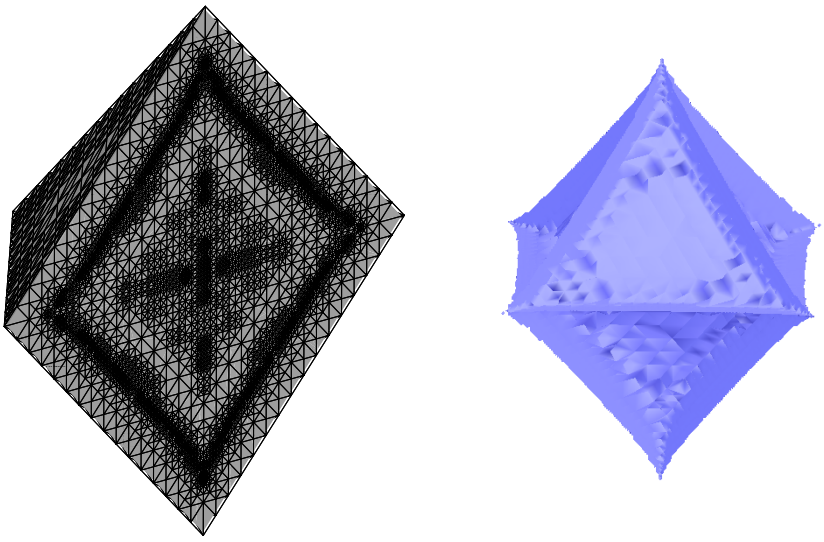

FIGURE 7.7. Example 7.4: Grid and $\partial\{u_h = \chi_h\}$ for $d = 3$ and adaptive iteration $j = 12$.

Figure 7.7 depicts the result for the same simulation in 3d. We display the grid on the boundary of $\Omega \cap \{x_2 \leq 0\}$ (left) and the set $\partial\{u_h = \chi_h\}$ (right) using the same viewpoint. We observe that in 3d the refinement close to the interface (curvilinear quadrilateral inside $\{x_2 = 0\}$) dominates that due to poor approximation of σ along the edges of the obstacle (cross inside $\{x_2 = 0\}$).

The second obstacle χ, which we consider only for $d = 2$, is again piecewise linear but with a downward peak:

$$\chi(x) := \operatorname{dist}(x, \partial\Omega) - 2\operatorname{dist}(x, \Omega\backslash\omega) - \tfrac{1}{5}$$

where $\omega = \{(x_1, x_2) \mid |x_1| + |x_2| < \frac{1}{4}\}$. We observe that the edges of χ contained in ω do not longer belong to the contact set, nor does the vertex of χ. We refer to Figure 7.8 where the obstacle and discrete solution are displayed in the sub-domain $\{x_1 \leq 0\}$ for ease of visualization. In contrast to the pyramid, σ is zero in ω.

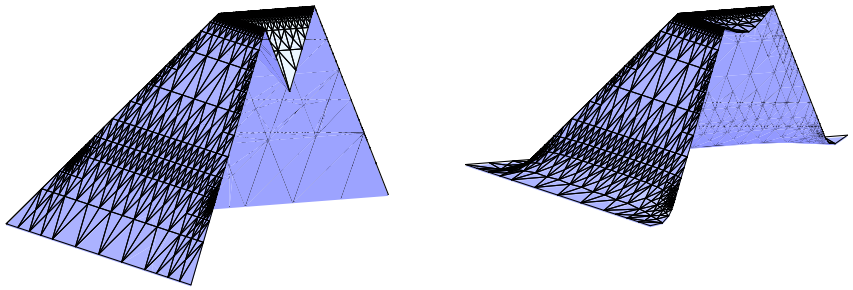

FIGURE 7.8. Example 7.4: Obstacle and discrete solution with corresponding adaptive grid on the domain $\{x_1 \leq 0\}$.

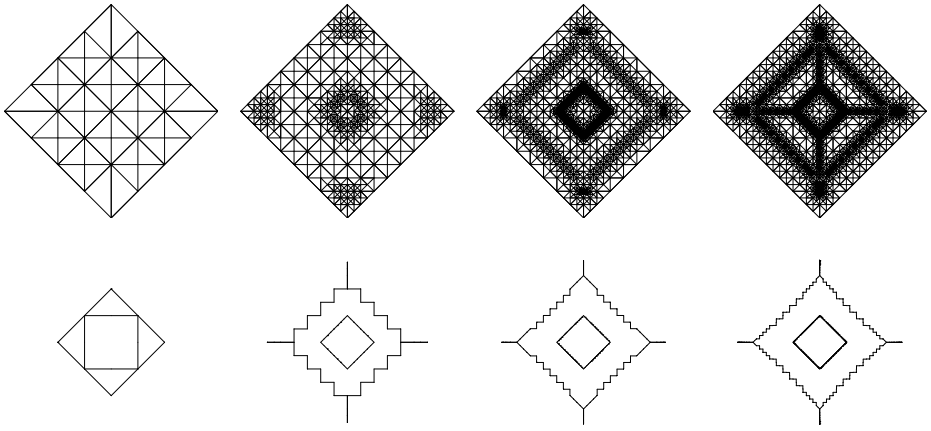

FIGURE 7.9. Example 7.4: Grids and $\partial\{u_h = \chi_h\}$ for adaptive iterations $j = 1, 4, 7, 10$.

This property of σ is reflected in the meshes of Figure 7.9: the refinement is concentrated on the interfaces, in particular $\partial\omega$, and the edges of χ but is rather coarse in ω because ω is not part of the contact set. Boundaries of the discrete set $\{u_h = \chi_h\}$ are also depicted.

References

[1] R. A. Adams, *Sobolev spaces*, vol. 65 of Pure and Applied Mathematics, Academic Press, Inc., a subsidiary of Harcourt Brace Jovanovich, Publishers, New York - San Francisco - London, 1975.

[2] C. Baiocchi, *Estimation d'erreur dans L^∞ pour les inèquations à obstacle*, in Mathematical Aspects of Finite Element Methods, Proc. Conf. Rome 1975, I. Galligani and E. Magenes, eds., vol. 606 of Lect. Notes Math., 1977, pp. 27–34.

[3] Z. Chen and R. H. Nochetto, *Residual type a posteriori error estimates for elliptic obstacle problems*, Numer. Math., 84 (2000), pp. 527–548.

[4] E. Dari, R. G. Durán, and C. Padra, *Maximum norm error estimators for three-dimensional elliptic problems*, SIAM J. Numer. Anal., 37 (2000), pp. 683–700.

[5] C. M. Elliott, *On the Finite Element Approximation of an Elliptic Variational Inequality Arising from an Implicit Time Discretization of the Stefan Problem*, IMA J. Numer. Anal., 1 (1981), pp. 115–125.

[6] L. C. Evans and R. Gariepy, *Measure Theory and Fine Properties of Functions*, Studies in Advanced Mathematics, CRC Press, Inc., 2000 Corporate Blvd., N.W., Boca Ratin, Florida, 33431, 1992.

[7] J. Frehse and U. Mosco, *Irregular obstacles and quasivariational inequalities of stochastic impulse control*, Ann. Scuola Norm. Sup. Cl. Pisa, 9 (1982), pp. 105–157.

[8] A. Friedman, *Variational Principles and Free-Boundary Problems*, Pure Appl. Math., John Wiley, New York, 1982.

[9] D. Kinderlehrer and G. Stampacchia, *An Introduction to Variational Inequalities and their Applications*, vol. 88 of Pure Appl. Math., Academic Press, New York, 1980.

[10] J. Nitsche, *L^∞ convergence of finite element approximations*, in Mathematical Aspects of Finite Element Methods, Proc. Conf. Rome 1975, I. Galligani and E. Magenes, eds., vol. 606 of Lectures Notes Math., 1977, pp. 261–274.

[11] R. H. Nochetto, *Pointwise a posteriori error estimates for elliptic problems on highly graded meshes*, Math. Comp., 64 (1995), pp. 1–22.

[12] R. H. Nochetto and L. B. Wahlbin, *Positivity preserving finite element approximation.* To appear in Math. Comp.

[13] J.-F. Rodrigues, *Obstacle Problems in Mathematical Physics*, vol. 134 of North-Holland Math. Stud., North-Holland, Amsterdam, 1987.

[14] A. Schatz and L. Wahlbin, *On the quasi-optimality in L^∞ of the H^1_0 projection into finite element spaces*, Math. Comp. 36 (1982), pp. 1–22.

[15] A. Schmidt and K.G. Siebert, *ALBERT — Software for Scientific Computations and Applications*, Acta Math. Univ. Comenianae 70 (2001), pp. 105–122.

[16] ———, *ALBERT: An adaptive hierarchical finite element toolbox*, Documentation, Preprint 06/2000 Universität Freiburg, 244 p.

[17] A. Veeser, *On A Posteriori Error Estimation for Constant Obstacle Problems* in Numerical Methods for Viscosity Solution and Applications, M. Falcone e C. Makridakis (ed.), World Scientific Publishing Company, Singapore, 2001.

[18] ———, *Efficient and reliable a posteriori error estimators for elliptic obstacle problems*, SIAM J. Numer. Anal., 39 (2001), pp. 146–167.

[19] R. Verfürth, *A Review of A Posteriori Error Estimation and Adaptive Mesh-Refinement Techniques*, Advances in Numerical Mathematics, John Wiley, Chichester, 1996.

Ricardo H. Nochetto, Department of Mathematics and Institute of Physical Science and Technology, University of Maryland, College Park, MD 20742, USA.

Partially supported by NSF Grant DMS-9971450 and NSF/DAAD Grant INT-9910086.

URL: `http://www.math.umd.edu/~rhn`

E-mail address: `rhn@math.umd.edu`

Kunibert G. Siebert, Institut für Angewandte Mathematik, Hermann-Herder-Str. 10, 79104 Freiburg, Germany.

Partially suported by DAAD/NSF grant "Projektbezogene Förderung des Wissenschaftleraustauschs in den Natur-, Ingenieur- und den Sozialwissenschaften mit der NSF".

URL: `http://www.mathematik.uni-freiburg.de/IAM/homepages/kunibert`

E-mail address: `kunibert@mathematik.uni-freiburg.de`

Andreas Veeser, Dipartimento di Matematica, Università degli Studi di Milano, Via C. Saldini 50, 20133 Milano, Italy.

Partially supported by DAAD/NSF grant "Projektbezogene Förderung des Wissenschaftleraustauschs in den Natur-, Ingenieur- und den Sozialwissenschaften mit der NSF" and by the TMR network "Viscosity solutions and their Applications".

E-mail address: `veeser@mat.unimi.it`